

# The geology and evolution of the Ballachulish Igneous Complex and Aureole

DAVID R.M. PATTISON<sup>1</sup> and BEN HARTE<sup>2</sup>

<sup>1</sup> *Department of Geology and Geophysics, University of Calgary, Calgary, Alberta, Canada T2N 1N4*

<sup>2</sup> *Department of Geology and Geophysics, The Grant Institute, University of Edinburgh, West Mains Road, Edinburgh, EH9 3JW*

## Synopsis

The Ballachulish Igneous Complex and Aureole is one of the world's most intensively studied plutonic–metamorphic complexes. The  $412 \pm 28$  Ma igneous complex was emplaced at a depth of about 10 km in regionally deformed and metamorphosed mica schists, quartzites and siliceous carbonates belonging to the Dalradian Supergroup. The intrusion is exposed over an area of  $c. 7.5 \times 4.5$  km<sup>2</sup> and is roughly cylinder-shaped to about 4 km beneath the surface, with the exception of two areas where the intrusion lies shallowly beneath the country rocks. The intrusion consists of an outer orthopyroxene-bearing diorite shell (emplacement temperature  $c. 1100^\circ\text{C}$ ) surrounding a central body of granite (emplacement temperature  $c. 850^\circ\text{C}$ ), the latter emplaced when the central portion of the diorite was still partially molten. A small, late leucocratic body in the centre of the granite is associated with weak Cu–Mo mineralization. The different intrusive phases represent separate magma batches which underwent little physical or chemical interaction during emplacement.

A well-developed contact aureole surrounds the intrusive complex. Isograds in pelitic rocks, the most abundant rock type in the aureole, can be mapped around the intrusion and range from development of cordierite 'spots' ( $c. 550^\circ\text{C}$ ) up to anatectic migmatization ( $700\text{--}800^\circ\text{C}$ ). Isograds in siliceous carbonates rocks range from development of talc ( $< 480^\circ\text{C}$ ) up to periclase formation ( $c. 750^\circ\text{C}$ ). In the quartzites, recrystallization and coarsening of clastic quartz occurs, and clastic feldspar grains develop a high-temperature structural state, as the contact is approached. The agreement of the sequence and spacing of isograds in pelites, siliceous carbonates and quartzites with equilibrium phase diagrams indicates no significant kinetic control on the positioning of isograds, although some metamorphic processes appear to have been kinetically controlled.

The contact metamorphism was mainly caused by intrusion of the diorite phase, with the later granite having little effect. Variations in width of the aureole are mainly due to variations in shape of the intrusion, temperature of the different intrusive phases, and the relative proportions of quartzite and pelite in the country rocks. The duration of the contact metamorphic event, for temperatures above conditions of the cordierite isograd ( $c. 550^\circ\text{C}$ ), was about 500 ka, whereas rocks were hot enough to be partially molten (temperatures above  $ca. 660^\circ\text{C}$ ) for about 270 ka. With the exception of some extensively fluid-fluxed partial melting on the west flank of the complex (Chaotic Zone), fluid communication between the intrusion and aureole was generally limited. Fluid fluxes in siliceous carbonates from the inner aureole on the east flank ranged from 100–1000 moles fluid cm<sup>-2</sup>. There is no evidence for the development of a large-scale hydrothermal circulation system.



## Introduction

The Ballachulish Igneous Complex and Aureole is one of the world's most comprehensively studied plutonic–metamorphic systems. It has received this attention because it represents a relatively simple intrusive complex emplaced in host rocks showing a wide range of lithologies, leading to a great diversity of products of contact metamorphism. In addition, the area is easily accessible and the exposure is generally excellent.

Two of the earliest references to the geology of the Ballachulish Complex are those of MacCulloch (1817) and MacKnight (1821): MacCulloch, an exponent of the

Huttonian view of geology, drew attention to the way in which the intrusive rocks metamorphosed the host mica schists, sent veins into them, and contained many fragments of the schists as inclusions, whereas MacKnight, who was influenced by Wernerian theories, viewed the contact-altered rocks around the intrusion as gneisses occupying their normal position in a granite – gneiss – mica slate – clay slate succession. Bailey and Maufe's (1916) memoir provided the first comprehensive summary of the geology of the igneous complex and aureole, largely based on work in the previous two decades by members of the Geological Survey. From 1981 to 1991, the Ballachulish Igneous Complex and Aureole was the focus of an international

multidisciplinary study examining equilibrium and kinetic processes in and around cooling plutons (Voll *et al.* 1991 and references therein). Since then, it has been used as a natural laboratory for investigating a range of igneous and metamorphic processes and to test new petrological techniques (e.g., Linklater 1990; Pattison 1992; Linklater *et al.* 1994; Ferry 1996*a, b*; Lind 1996; Holness 1997). The results of these studies have allowed an unusually detailed understanding of the physical and temporal evolution of the igneous complex and aureole such that, in a broader sense, the complex may serve as a type example of the intrusive process at moderate crustal depths.

The Ballachulish Igneous Complex and aureole are located in Argyllshire, west Scotland, at the SE junction of Lochs Linnhe and Leven (Fig. 1). The igneous complex is emplaced in deformed and regionally metamorphosed sediments of lower–middle sections of the Dalradian Supergroup. The age of the complex is  $412 \pm 28$  Ma (Weiss 1986; Troll and Weiss 1991) and, alongside other complexes such as those of Glen Coe, Etive and Ben Nevis, is part of the Argyll suite of granitoid intrusions of the west-central Scottish Highlands (Bailey and Maufe 1960; Stephens and Halliday 1984). The Argyll suite itself is part of the extensive Siluro-Devonian (c. 430–400 Ma) Caledonian intrusive series found throughout Scotland. The Argyll intrusions are classified as ‘Newer’ or ‘late’ granitoids, owing to their emplacement subsequent to regional deformation and metamorphic events affecting the Dalradian Supergroup in the Grampian Highlands (Harte and Voll 1991). The present erosion level at Ballachulish reveals rocks emplaced at a relatively deep crustal level (c. 10 km), without volcanic sequences such as those found at Glen Coe and Ben Nevis.

The purpose of this contribution is to provide a synthesis of the geology and evolution of the Ballachulish Igneous Complex and Aureole, and bring out some of the wider implications of the studies of the complex, including: the extent and timing of fluid movement; the thermal evolution of the aureole in relation to the intrusive events; and an assessment of equilibrium and kinetic controls on isograd development.

### Geological setting of the Ballachulish Complex

#### Dalradian metasedimentary units

The distribution and stratigraphic order (Litherland 1980) of the Dalradian lithological units which form the country rocks to the intrusion are shown in Figure 1, together with aspects of their regional structure and metamorphic grade (see Pattison and Voll 1991, and references therein, for further details). Owing to the fact that the Dalradian rocks have undergone regional and contact metamorphism to different degrees, the rock types of the different metasedimentary units vary considerably throughout the area (e.g., phyllite *v.* hornfels, etc.). In this paper, we refer to the lithological units according to the descriptive terminology established by Bailey and Maufe (1960) and Litherland (1980), which are based on the occurrence of the rocks outside of the aureole.

The oldest stratigraphic unit found in the aureole is the Leven Schist, comprising grey-green phyllites and thinly bedded metasiltsstones, dirty quartzites and variably graphitic slates. The overlying Ballachulish Limestone comprises a lower member of calcareous schist with dolomitic interbeds and an upper member of dark, graphitic marble. The Ballachulish Limestone is succeeded upwards by the Ballachulish Slate, a dark grey, graphitic slate with some silty layers and locally abundant pyrite (outside aureole) and pyrrhotite (inside aureole). Between the Ballachulish Slate and the younger Appin Quartzite is a unit known as the Transition Series, which grades upwards from graphitic phyllite with thin quartzite interbeds near the base, to quartzite with thin graphitic phyllite interbeds near the top.

The Appin Quartzite is a white to grey, medium- to coarse-grained feldspathic quartzite commonly showing prominent cross-bedding and grading. The Appin Limestone and Appin Phyllite comprise somewhat repetitive interlayered units with a higher proportion of limestone towards the lower boundary with the Appin Quartzite. The ‘limestone’ ranges upwards from relatively pure dolomite and marble near the bottom of the unit to impure dolomites and calcareous phyllites interbedded with phyllite layers. The ‘phyllite’ parts of the unit comprises phyllite and micaceous meta-sandstones variably interbedded with quartzitic layers, with the latter typically showing good cross bedding and graded bedding. The Cuil Bay Slate is a dark grey, graphitic slate with rare millimetre–centimetre-scale interbeds of graded quartzite.

The succession from Leven Schist to Cuil Bay Slate is part of the Appin Group. Overlying the Appin Group are rocks of the Creran Succession, which were originally included by Bailey and Maufe (1960) in the Leven Schist, but were reassigned to the stratigraphically overlying Argyll Group by Litherland (1980). The Creran Succession comprises thinly bedded flags and striped, variably graphitic phyllites; their similarity to the Leven Schist led to Bailey’s old name of ‘Banded Series of Leven Schists’. The outcrop of the Creran Succession is bounded by slides, of which the Benderloch Slide (Fig. 1) appears to roughly coincide with a syn-sedimentary depositional fault line that was reactivated during the earliest phase of Dalradian deformation ( $D_1$ ) (Litherland 1980, 1982).

No fossils have been found in the Appin–Argyll stratigraphic sequence. A high precision zircon age date of  $590 \pm 2$  Ma for the Ben Vuirich granite (Rogers *et al.* 1989) restricts the depositional age of the Appin and Argyll Group rocks to the late Proterozoic or earlier. The age(s) of major regional deformation and metamorphism of the Grampian Orogeny of the Dalradian are uncertain (e.g. Tanner 1995), but are probably in the Middle Cambrian to Middle Ordovician range.

#### Regional structure

Prior to the intrusion of the igneous complex, extensive major deformation belonging to the  $D_1$  episode of Roberts (1976) affected the host rocks and formed the series of major NE–SW-trending folds and slides (ductile thrust

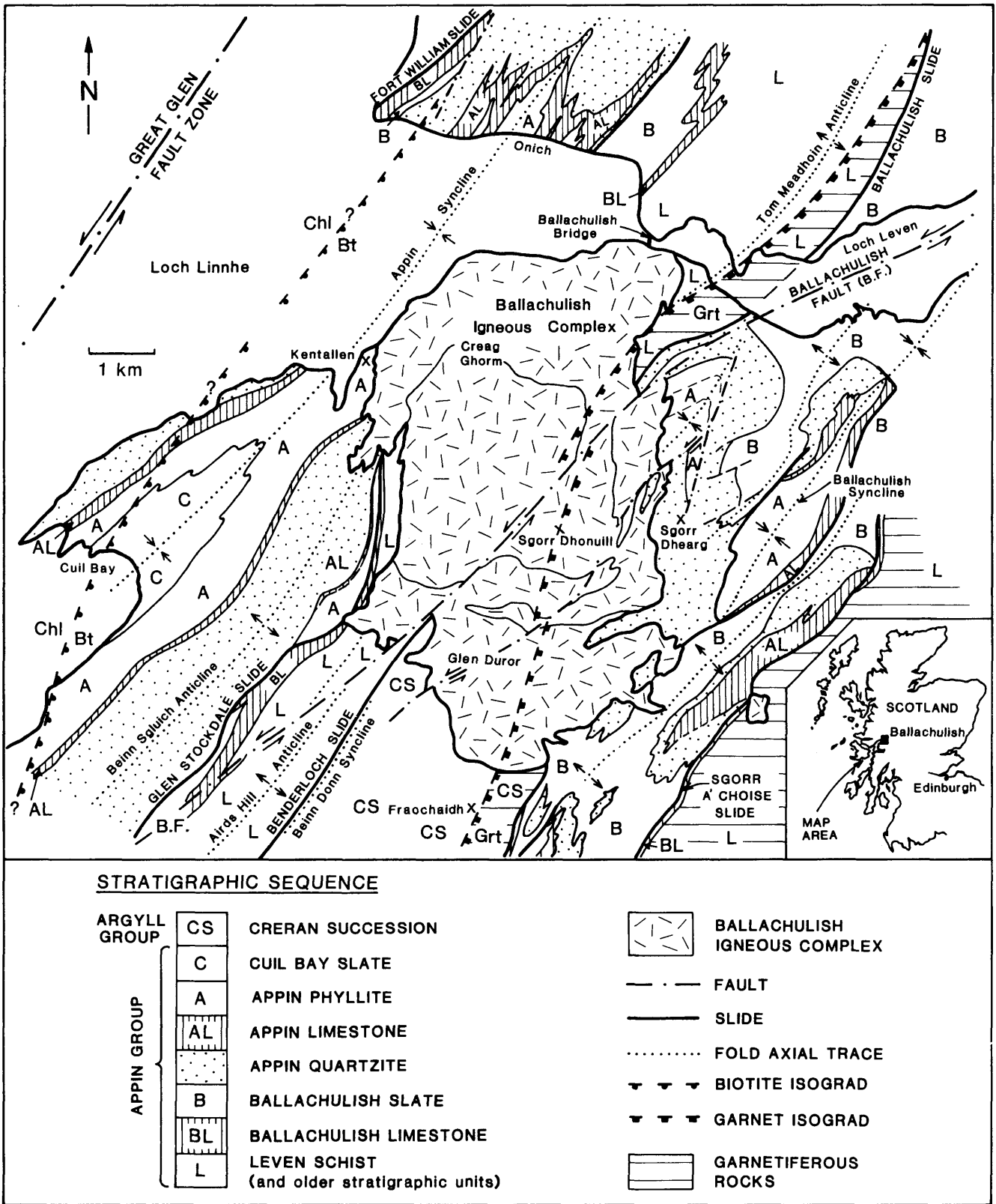
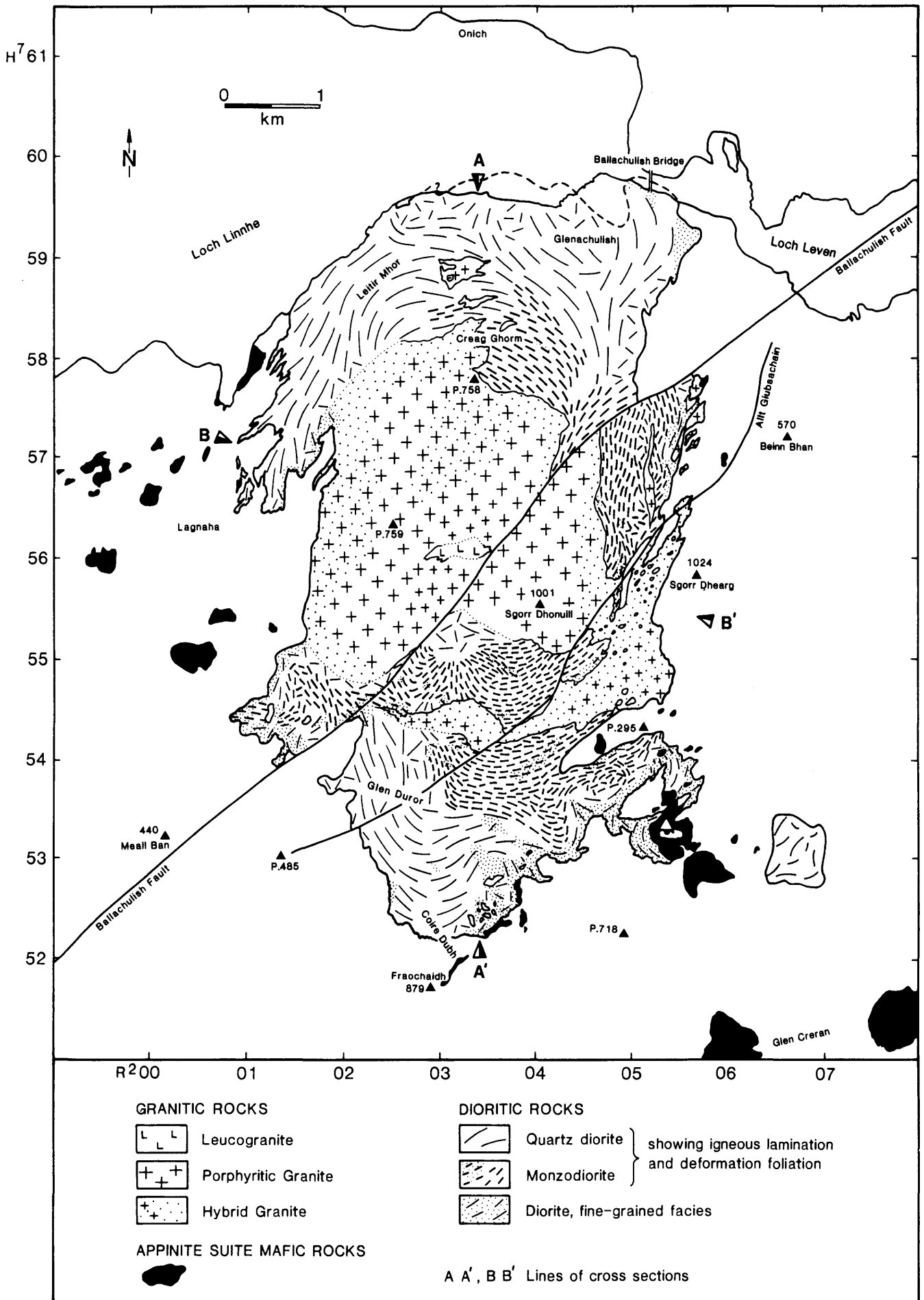


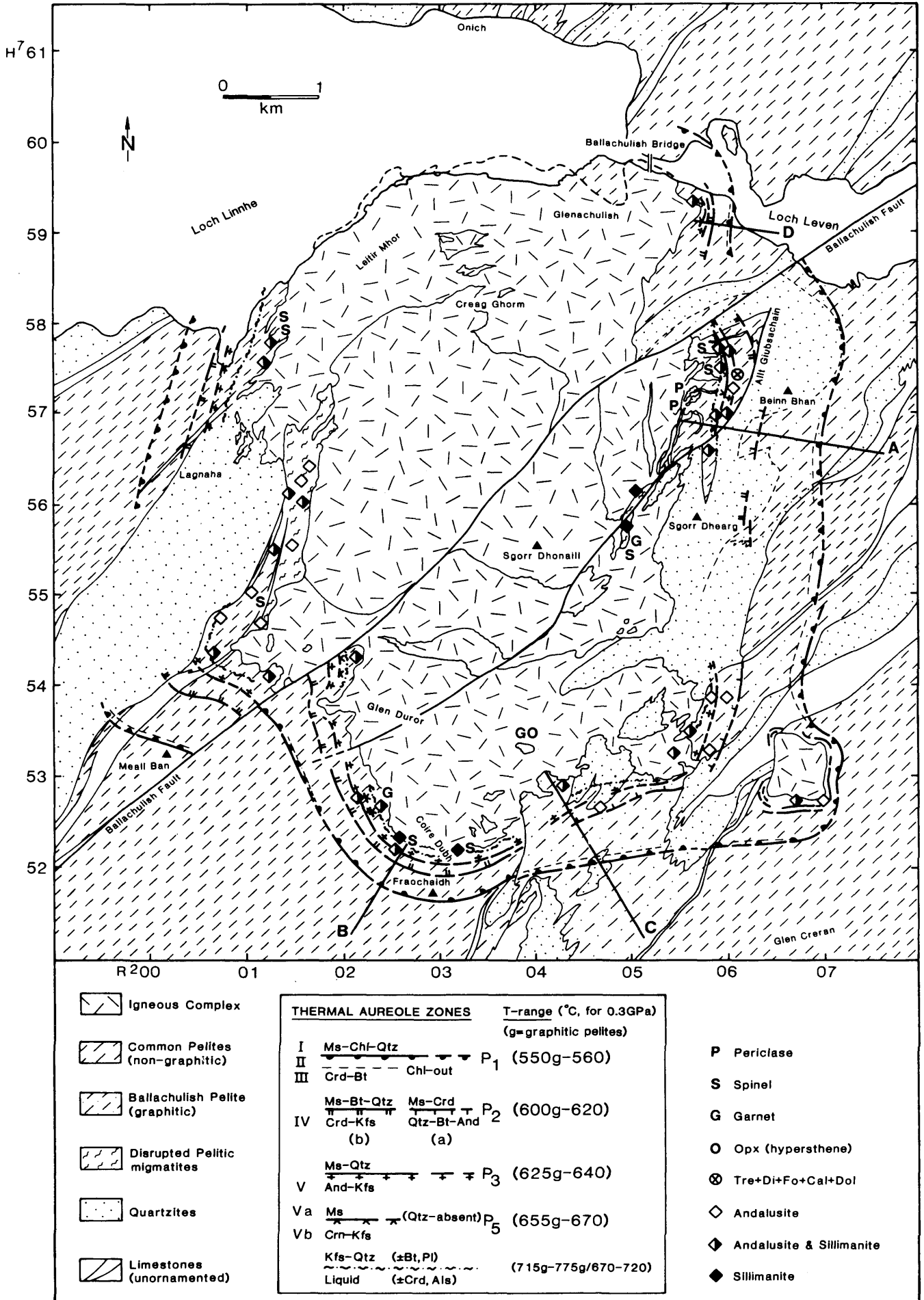
FIG. 1. (above). Map showing the setting of the Ballachulish Igneous Complex and Aureole, with regional lithostratigraphy, structure and metamorphism of the surrounding country rocks (modified from Pattison and Voll 1991). The position of garnet isograd has been extrapolated through the igneous complex. Inset shows position of Ballachulish Complex in the Scottish Highlands and Islands.

FIG. 2. (overleaf). Geological map of the Ballachulish Igneous Complex (modified from Weiss 1986 and Map 2 in Voll *et al.* (1991)). Cross-sections A-A' and B-B' are shown in Fig. 4.

FIG. 3. (overleaf). Pelitic contact metamorphic zones and isograds in the contact aureole, together with the distribution of other key minerals (modified from Pattison 1992, and from Map 2 in Voll *et al.* 1991). The extensive area of disrupted migmatites shown on the west side of the igneous complex is referred to as the Chaotic Zone. Lines A, B, C and D give the positions of transects for the thermal profiles in Figs. 11 and 12. Appinites are not shown (see Fig. 2).



BALLACHULISH IGNEOUS COMPLEX and AUREOLE



- Igneous Complex
- Common Pelites (non-graphitic)
- Ballachulish Pelite (graphitic)
- Disrupted Pelitic migmatites
- Quartzites
- Limestones (unornamented)

THERMAL AUREOLE ZONES		T-range (°C, for 0.3GPa)
I	Ms-Chl-Qtz	(550g-560)
II	Crld-Bt	P <sub>1</sub>
III	Chl-out	
IV	Ms-Bt-Qtz	P <sub>2</sub> (600g-620)
	Crld-Kfs	
	(b)	(a)
V	Ms-Qtz	P <sub>3</sub> (625g-640)
	And-Kfs	
Va	Ms	P <sub>5</sub> (655g-670)
	(Qtz-absent)	
Vb	Crn-Kfs	
	Kfs-Qtz (±Bt, Pl)	(715g-775g/670-720)
	Liquid (±Crld, Als)	

- P Periclase
- S Spinel
- G Garnet
- O Opx (hypersthene)
- ⊗ Tre+Di+Fo+Cal+Dol
- ◇ Andalusite
- ◊ Andalusite & Sillimanite
- ◆ Sillimanite

faults that were active early in the orogenic history) shown in Figure 1 (Pattison and Voll 1991). The folds are tight and generally upright and plunge shallowly NE or SW (with the exception of the steeply SW-plunging Coire Giubhsachain syncline on the NE flank of the igneous complex). Small-scale deformation features associated with  $D_1$  include tight to isoclinal parasitic folds, and a prominent, steeply dipping, NE-SW-striking, penetrative axial-planar slaty cleavage in micaceous units which is typically sub-parallel to bedding.

At many localities, strong strain-slip and/or crenulation cleavages overprint the early ( $D_1$ ) slaty cleavage, and in most cases this secondary cleavage is probably associated with a second set of large scale folds which also strike NE-SW, represented by the Stob Ban synform to the NE of the area (Roberts 1976). Later deformation episodes are manifested in a variety of millimetre- to metre-scale features affecting primary layering and early cleavage, such as folds, kink bands, crenulations and crenulation cleavages at various orientations. Roberts (1976) and Roberts and Treagus (1977) provide further details on pre-intrusion structural relations in the area.

Crosscutting the igneous complex and aureole is the NE-SW Ballachulish strike-slip fault (Figs. 1, 2 and 3), which has a post-intrusion sinistral displacement of 600–800 m (Pattison 1985; Weiss 1986). The Ballachulish Fault is marked along its length by crushed and shattered rock, and has a prominent physiographic expression. To the NE it is linked by aligned 'shatter belts' (Bailey and Maufe 1960) to a wrench fault west of Loch Laggan identified on Landsat imagery by Johnson and Frost (1977), which is probably the same as the Laggan Dam fault of Anderson (1956). Along the line of shatter belts, sinistral displacements of 0.5–1.5 km (Hickman 1975; Pattison 1985) are comparable to those in the Ballachulish area, giving a total fault length of at least 80 km (Pattison 1985). To the SW of the igneous complex, the Ballachulish Fault continues in a NE-SW direction (Hickman 1975; Pattison 1985) and therefore diverges from, rather than joins with, the speculated trace of the Pass of Brander fault shown in the maps of Litherland (1980, 1982) and Treagus (1991). We find no evidence on the ground for the proposed 'Ballachulish-Corrieyairack' shear zone of Jacques and Reavy (1994).

The Ballachulish Fault makes about a 15° angle with the nearby Great Glen Fault Zone, and may be a splay off this fault zone (Johnson and Frost 1977). Some fault rocks have been affected by contact metamorphism, suggesting that the Ballachulish Fault was active before as well as after emplacement of the Ballachulish Igneous Complex. Weiss and Troll (1991) suggested that strike-slip movement along the Ballachulish Fault may have facilitated emplacement of the igneous complex.

### Regional metamorphism

Pre-intrusion regional metamorphic grade increases from NW to SE across the area from chlorite ± biotite grade to garnet grade (Pattison and Voll 1991 and references therein). The regional metamorphic zones and

isograds shown on Figure 1 are interpreted as the low-grade portion of a Barrovian metamorphic sequence (Atherton 1977; Fettes et al. 1985), probably associated with the regional Grampian Dalradian metamorphic event dated at 520–490 Ma (Dempster 1985; Harte 1988; but see also Tanner 1995). Regional metamorphic temperatures have been estimated to range from *c.* 400°C in the NW to *c.* 550°C in the SE, at pressures of *c.* 5–7 kbar (equivalent to 17–23 km depth) (Pattison and Voll 1991).

In the west of the area, along the north shore of Loch Leven and on Ardsheal Peninsula, interbedded layers with and without biotite attest to the importance of bulk composition in controlling the development of biotite, and makes uncertain the delineation of distinct chlorite and biotite zones such as was done by Elles and Tilley (1930) and Atherton (1977). The distribution of garnet in the area is also complex (Fig. 1). Going from NW to SE, the garnet zone first occurs in the Leven Schist and Creran Succession at the isograd shown in Figure 1, extending from about 1 km west of Ballachulish Bridge in the north of the area to just east of the summit of Fraochaidh in the south. To the east of this isograd garnet occurs in a 500–700 m wide NE-SW-trending 'strip', but with much of its extent cut out by the Igneous Complex. To the east of this garnet-bearing strip, across the Ballachulish Slide, is a garnet-absent interval occupied by the Appin Limestone/Phyllite and especially Ballachulish Slate lithologies, until further east garnet reappears simultaneously with the re-appearance of the Leven Schist.

This unusual pattern with the abrupt disappearance of garnet across the Ballachulish Slide, particularly well seen on the north shore of Loch Leven, was a point of debate between Bailey (1923, and in Bailey and Maufe 1960) and Elles and Tilley (1930). Bailey considered that the Ballachulish Slide predated metamorphism and that the abrupt disappearance of garnet across the slide as one entered the Appin Limestone/Phyllite and Ballachulish Slate was due to the change of bulk composition of the rocks. Elles and Tilley (1930), in contrast, thought that the change in garnet occurrence indicated a difference in metamorphic grade of the rocks on either side of the Ballachulish Slide, implying that the slide juxtaposed rocks of different grade and post-dated the metamorphism. Mineral composition analysis indicates that variation in bulk composition can explain the irregular distribution of garnet east of the garnet isograd (Pattison and Voll 1991), a view consistent with several other lines of evidence indicating that metamorphism post-dated sliding (Bailey and Maufe 1960; Roberts 1976; Atherton 1977; Pattison and Voll 1991; Pattison and Harte 1994).

### Small pre-intrusion igneous bodies

Several small explosion-breccia pipes and mafic-ultramafic intrusions (Fig. 2), collectively known as the Appinite Suite (Bowes and Wright 1967), were emplaced prior to the Ballachulish Igneous Complex but following regional deformation and metamorphism. These intrusions include a number of sub-types (e.g. kentallenite) characterized by generally coarse grain size and consisting of

variable proportions of olivine, augite, hypersthene, hornblende, biotite, plagioclase, K-feldspar and quartz. Based on their textures and major- and trace-element analyses, Wright and Bowes (1979) concluded that the bodies represent differentiates of a volatile, basic magma of mantle origin. Weiss and Troll (1989) noted a hybrid transition zone between a large appinite body and quartz diorite on the complex's SE margin, suggesting that the appinite bodies were emplaced only shortly before the main igneous complex.

### Uplift and erosion

Following attainment of regional metamorphic P–T conditions at approximately 520–490 Ma, the Dalradian host rocks were uplifted, and at the time of intrusion of the igneous complex ( $412 \pm 28$  Ma) were at a depth of about 10 km (3 kbar). The ambient country rock temperature prior to emplacement is estimated to have been about 250 °C (Pattison and Voll 1991).

No major tilting occurred following emplacement of the Ballachulish Complex. The Lorne Lavas, occurring about 15 km south of the Ballachulish Complex and forming the largest preserved volcanic sequence of Siluro-Devonian igneous activity, are close to flat lying. Droop and Treloar (1981) estimated a maximum tilting of 3 km over 35 km along a NW–SE axis in the Etive Complex, 8 km SE of Ballachulish. Assuming the same amount of tilting, this translates to a maximum differential uplift of 0.7 km across the 8 km width of the Ballachulish Complex and Aureole, which is less than the 1 km topographic relief in the area.

### The Ballachulish Igneous Complex

The igneous complex covers an area of about  $7.5 \times 4.5$  km<sup>2</sup>, and consists of a zoned monzodiorite–quartz diorite envelope with flow- and deformation-foliation surrounding a core of variably porphyritic granite with hybrid margins (Fig. 2) (Weiss 1986, 1991; Weiss and Troll 1989; 1991; Troll and Weiss 1991). To the SE of the complex is a small quartz diorite satellite intrusion probably related to the main intrusion.

### Rock types

The igneous complex shows a range of intrusive rocks (Fig. 2), but three main types predominate using the IUGS classification scheme (Weiss and Troll 1989).

(1) Monzodiorites. These include: a central 'dry' facies of hypersthene-augite monzodiorites containing <2.5% quartz and <6% biotite and amphibole; and a central 'hydrated' facies of hypersthene-augite-quartz monzodiorites with >3% quartz and 14–26% biotite and amphibole.

(2) Quartz diorites. These include: augite-amphibole quartz diorites with >20% mafic minerals and >1.5% augite; biotite-amphibole quartz diorites with <1.5% augite; and leucocratic biotite-amphibole quartz diorites with <20% mafic minerals.

(3) Granites. These include biotite-bearing granodiorites, weakly porphyritic granites, quartz monzodiorites

(hybrid marginal facies) and fine-grained monzogranite (leucogranite), the latter associated with hydrothermal alteration and weak Cu–Mo mineralization.

The monzodiorites and quartz diorites (1 and 2) together comprise the outer diorite envelope of the igneous complex, whereas the granitic rocks (3) comprise the central granite core (Fig. 2).

*Monzodiorite–quartz diorite envelope.* Greenish-grey pyroxene monzodiorites form the inner part of the diorite envelope, occupying a roughly crescent-shaped area. A fine-grained marginal facies of this rock suggests that the monzodiorite magma intruded in a largely liquid state. Away from the margins, the monzodiorites are equigranular with an adcumulus texture of andesine, augite, hypersthene and apatite phenocrysts with intercumulus opaque oxides and K-feldspar. Coarse-grained, black, Ti-rich poikilitic biotite is conspicuous in the hypersthene-bearing monzodiorites. Minor secondary hornblende is common. The K-feldspar is typically crypto- to micro-perthitic, indicating that these rocks cooled in a mainly dry, fluid-absent environment. Ilmenite and magnetite occur in a ratio of about 2:1. The monzodiorite-quartz diorite rocks show evidence of igneous flow lamination and deformation foliation, with orientations as shown on Figure 2 and discussed further below.

Grey quartz diorites form the marginal northern, north-western and southern parts of the diorite envelope. Junctions of quartz diorite with monzodiorite, and between fine-grained and coarse-grained types of quartz diorite, range from sharp to gradational. Grain size is highly variable, especially in the more leucocratic parts in which metasedimentary xenoliths are abundant. In the more homogeneous 'normal facies' of the quartz diorites, biotite is the main mafic phase, accompanied by greenish amphibole, often with core relicts of augite. In contrast to the monzodiorites, plagioclase is complexly zoned. Poikilitic K-feldspars reach a diameter of 0.5–1 cm, and may be optically homogeneous or contain patch- and flame-perthite structures, the latter suggestive of deuteric coarsening favoured by the presence of fluids during cooling.

*Granite core.* The main granite core is exposed over an area of about 8 km<sup>2</sup> (Fig. 2) and is relatively homogeneous. Reddish K-feldspar phenocrysts, 0.5–1.5 cm in length and comprising 5–15 vol.% of the rock, form euhedral-subhedral crystals whose margins merge into the granodioritic groundmass. The K-feldspar shows patch- to vein-perthite structures. Biotite and amphibole, the latter often with relict augite cores, are the main mafic phases.

*Leucogranite stock and associated hydrothermal alteration and disseminated Cu–Mo mineralization.* A small non-porphyrific, fine-grained, muscovite-bearing leucogranite stock occurs in the the centre of the granite core (Fig. 2). Spatially associated with the stock is a zone of hydrothermal alteration (mainly sericitization) of variable intensity,

in addition to low grade disseminated Cu–Mo mineralization, the latter too poorly developed to be of economic interest (Haslam and Kimbell 1981). The altered and mineralized zone occurs partly in the host granite and partly in the leucogranite, comprising a weakly developed stockwork of sub-millimetre to rarely millimetre-wide quartz veins containing variable proportions of pyrite, chalcopyrite and molybdenite. The style of alteration and mineralization bears similarities to economic Cu–Mo porphyry systems, only on a much smaller scale.

**Dykes.** Rare 1.5 to 5 m wide rhyolite dykes, sometimes with quartz and K-feldspar phenocrysts, cut the diorites and granites, dipping towards the centre of the complex. Late microdiorite dykes, most likely members of the Etive and Ben Nevis swarms (Bailey and Maufe 1960), cut all magmatic and metasedimentary units of the Ballachulish area.

#### Contact relations and geophysics

Two cross-sections through the igneous complex are shown in Figure 4. The contacts between the igneous complex and metasediments are generally sharp and discordant, and follow a variety of lithological or structural anisotropies comprising bedding planes, the main cleavage, a set of NNE and SE joints, and rarely NE-trending fault

zones. The overall lack of deflections of bedding and absence of concentric tectonic fabrics in the marginal host rocks suggest that there was no significant pushing aside or upward or downward flow of the host rocks to accommodate the volume of emplaced magma. The one location where there is possible evidence of deflection of bedding adjacent to the intrusion is in the north part of the Chaotic Zone on the west flank.

Internal contact zones between different phases of the igneous complex vary. Sharp, well-defined contacts are found in the middle and eastern parts of the complex where the granites cut the monzodiorites. In contrast, in the southwestern and especially northwestern parts of the complex, hybrid transitional zones up to 500 m wide separate quartz diorites from the later granites. The contrast between the sharp granite-monzodiorite contacts and gradational granite–quartz diorite contacts suggest that the ‘dry’ monzodiorite was largely consolidated at the time of granite intrusion, whereas the more fractionated quartz diorite was only partially consolidated, resulting in magma mixing and the production of the hybrid transition zone. Granite apophyses generally have the form of incomplete ring dykes, thinning and flattening upwards and dipping away from the centre of the complex (Fig. 4). The fine grained leucogranite shows sharp contacts as well as diffuse transition zones with the surrounding porphyritic granite; semicircular, gently dipping internal contact zones indicate a possible hood shape for the leucogranite (Fig. 4).

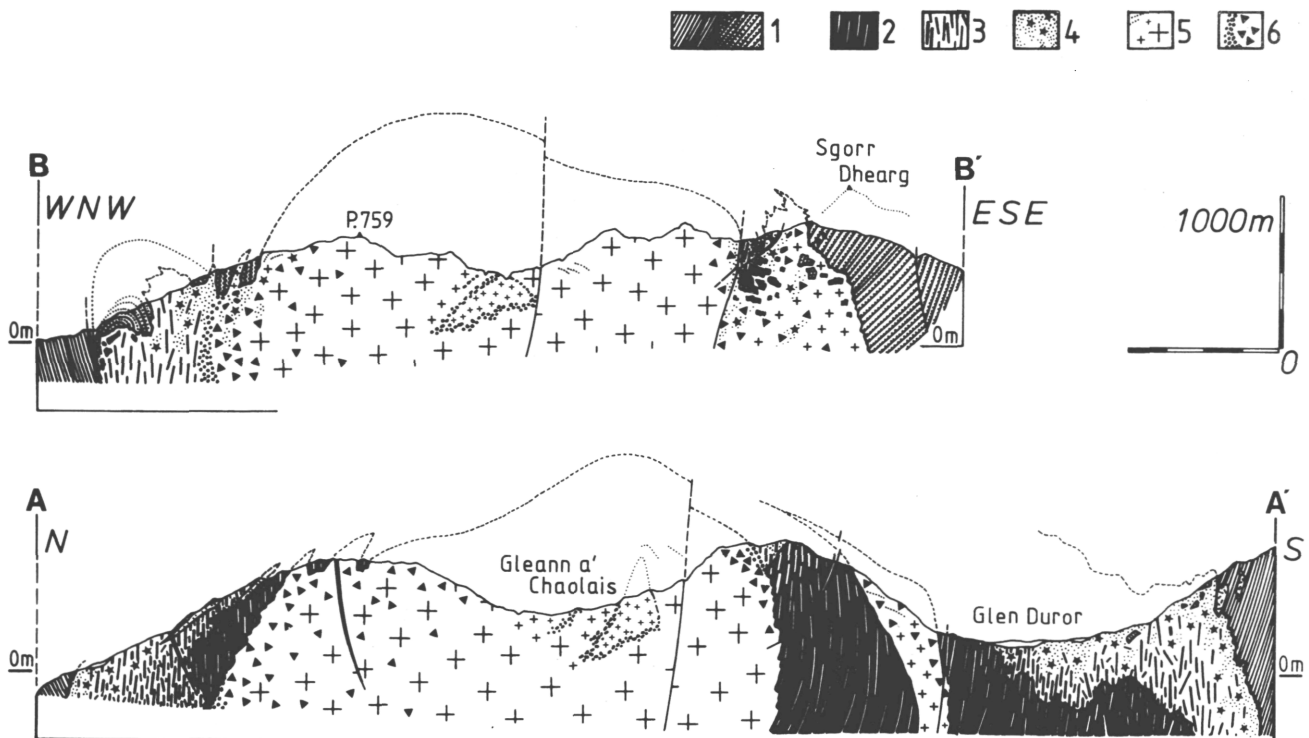


FIG 4. Geological cross-sections through the igneous complex (see section lines in Fig. 2), from Weiss (1986) and Troll and Weiss (1991). 1, Metasediments. *Lined pattern* indicates pelites and semipelites; *lined pattern with dots* represents quartzites. *Squiggly lines* indicated migmatitic rocks. The orientation of the lines gives the attitude of the bedding projected into the cross section. 2, Monzodiorites, showing flow- and deformation-foliation. 3, Quartz diorites, showing alignment of metasedimentary xenoliths. 4, Fine-grained diorites with xenoliths. 5, Granites. The fine crossed ornament in the centre represents leucogranite, bounded by a stippled margin representing a gradational contact with the main granite. 6, Hybrid transition zones between granite and quartz diorite. The dotted line labelled ‘Sgorr Dhearg’ represents the projected topographic expression of this peak which occurs about 300m N of the line of section.

Aeromagnetic patterns reveal a striking anomaly over the Ballachulish Complex (Rabbel and Meissner 1991). Based on a variety of models and optimization techniques, Rabbel and Meissner estimated that the minimum depth extent of the complex was 4 km. The aeromagnetic data indicate that the western and southeastern diorites of the complex spread laterally 0.5–1.5 km below the metamorphic country rocks, consistent with the following geological features: the shape of the margins of the complex in the west and SE (Fig. 2); the development of an unusually extensive zone of disrupted migmatites in the western aureole; and a broadening of the metamorphic aureole in the SE (Fig. 3). On the western margin, quartz diorite intruded and partially filled the large quartzite anticline (Beinn Sgluich anticline), producing a roof zone to the quartz diorite between the quartzite anticline and the igneous complex. In the SE part of the complex, quartz diorite extends south-eastwards under the exposed metasedimentary rocks towards the small satellite intrusion, producing a roof zone in between the exposed intrusive rocks. A surface magnetic survey over the southern portion of the complex reveals steep (70–90°), outwardly dipping contacts down to about 400 m depth, consistent with the field evidence.

The igneous complex has only a weak gravity anomaly, indicating a small density contrast between the pluton and its surroundings (Rabbel and Meissner 1991). Lack of significant gravity contrasts between the central granite and diorite shell suggest that the central granite grades into diorite at relatively shallow depths.

#### Xenoliths and screens

Numerous metasedimentary (pelite, quartzite, marble/calcsilicate) and mafic xenoliths are present in the outer quartz-bearing diorites, especially along the NW margin of the complex where quartz diorites contain abundant xenoliths in various stages of resorption. The abundance of xenoliths at the margins of the quartz diorites is attributed to piecemeal stoping. In contrast, xenoliths are rare in the inner, hypersthene-rich monzodiorites. The central granite contains a few xenoliths around its margins, most commonly in the hybrid mixing zones with the quartz diorites.

Pelitic xenoliths are typically high grade cordierite-rich hornfelses of a similar texture and mineralogy to those in the aureole. Progressive absorption by melting and disintegration converted many xenoliths to dark schlieren rich in cordierite, magnetite and plagioclase. Mafic xenoliths of hornblende ± pyroxene-rich material are most likely fragments of Appinite suite mafic rocks, or fragments of early crystallized hypersthene monzodiorite that fell back into the fractionating magma.

Along the eastern contact, on the western and north-western slopes of Sgorr Dhearg, hybrid granites enclose a large (750 m long) quartzite screen and numerous rafts of marbles, calc-silicates and partially disaggregated pelitic sediments (Figs. 2 and 3). Except for some minor tilting, the relative coherency and consistent orientation of the rafts suggest preservation of the near-pre-intrusive orientation. In contrast, in the southeastern portion of the

complex where quartz diorite dips shallowly under the adjacent metasediments, the random orientation of metasedimentary rafts up to 250 m in length suggests disintegration of a metasedimentary roof zone by block stoping.

#### Flow- and deformation-foliation

Mapping of planar orientations of tabular phenocrysts, schlieren and xenoliths was used to trace directions of magmatic flow in the igneous complex (Weiss and Troll 1991). The planar fabrics are shown in Fig. 2 by curving patterns. In the monzodiorites, phenocrysts of plagioclase, augite and hypersthene define planar orientations dipping vertically or steeply towards the centre of the complex at 75–85°. These alignments are thought to be due to magmatic flow involving megascopic convection currents, and give an overall impression of a steep cone-sheet. A weak deformation foliation superimposed on the primary magmatic foliation is revealed by bent biotite crystals and plagioclase crystals showing bending, marginal subgrain development and/or mechanical twinning. These deformation features are ascribed to the later emplacement and possible ballooning of the central granite, resulting in stress being transmitted through the plagioclase-dominated crystal framework of the largely consolidated monzodiorites.

In the quartz diorites, tabular xenoliths and schlieren show a wider range of orientations, usually dipping at 50–85° towards the margins of the igneous complex. These orientations are attributed to laminar flow in a partly crystallized magma (Weiss and Troll 1991). The transition between the regular magmatic flow foliations in the monzodiorites to the more irregular orientations in the quartz diorites may have been due to changes in rheology from both continued fractional crystallization and country rock assimilation in the outer portions of the diorite magma. Deflections of magmatic flow around irregular blocky roof structures and subsiding country rocks rafts may also have played a part. The deformation features noted in the monzodiorites are not seen in the quartz diorites, possibly due to emplacement of the central granite when the partially consolidated quartz diorite was a liquid-supported magma, consistent with the development of hybrid mixing zones between granite and quartz diorite.

In the granites, a poorly developed preferred orientation of K-feldspar phenocrysts is only visible in marginal parts, suggesting emplacement of the granite magma as a viscous crystal mush diapir already containing phenocrysts of plagioclase, biotite and K-feldspar in random orientation.

#### Whole rock geochemistry of intrusive rocks

Weiss and Troll (1989) and Troll and Weiss (1991) did a detailed geochemical study of the intrusive rock types. In a total alkalis/silica diagram, monzodiorites plot on or slightly to the alkaline side of the alkaline/subalkaline dividing line, whereas all quartz diorites and granites are subalkaline. Monzodiorites, quartz diorites and granites define a nearly straight calc-alkaline trend lacking any significant iron enrichment. Using the mole fraction  $X_{\text{ALK}} [= \text{Al}_2\text{O}_3/(\text{Na}_2\text{O} + \text{K}_2\text{O} + 0.5 \times \text{CaO})]$  in Pitcher's (1982)

geotectonic classification scheme, the monzodiorites plot as meta-aluminous Caledonian 'igneous (I)-type' magmas, the metasediment-contaminated quartz diorites plot as transitional to peraluminous crustally derived magmas, and the granites plot as 'sediment (S)-type' granitoids derived by crustal melting. REE concentrations in monzodiorites and granites are similar, suggesting that the geochemical signature of the two main magma batches was imposed from the source region rather than from fractional crystallization of one large magma batch. Based on absolute abundances and ratios of a number of REE, batch melting of a significant lower crustal component involving intermediate granulites or gneisses is implicated in the production of the monzodiorite–quartz diorite magma.

Contrasts in the Thornton and Tuttle (1960) differentiation index (D.I.) between the monzodiorite–quartz diorite envelope (D.I.  $\approx$  45–70) and granite core (D.I.  $\approx$  80  $\pm$  2.5) suggest different extents of fractional crystallization within the two magma batches. The large differentiation range in the diorite suite indicates effective fractionation, possibly favoured by magma convection and accumulate consolidation, whereas the restricted compositional range of granites is attributed to consolidation from a 'crystal mush' with relatively restricted separation of cumulus phases and viscous intercumulus liquid.

Within the diorite suite, Zr and Sr depletions in the leucocratic quartz diorites indicate about 25% assimilation of pelitic material, which accords with the abundance of partially digested metasedimentary xenoliths. Within the granites, leucogranites are strongly depleted in Sr, Zn, F and Li, indicating separation of an aqueous fluid at the end stages of crystallization, consistent with the hydrothermal alteration haloe and disseminated Cu–Mo mineralisation localized around the leucogranite in the centre of the complex (Haslam and Kimbell 1981).

#### Stable isotope compositions of intrusive rocks

Hoernes *et al.* (1991) investigated the stable isotope geochemistry of the igneous complex. Whole rock  $\delta^{18}\text{O}$  and  $\delta\text{D}$  values of rocks from the igneous complex range from +7.5 to +10.9 ‰ and –73 to –48 ‰ respectively. The granites tend to be enriched in  $\delta^{18}\text{O}$  relative to the monzodiorite–quartz diorite suite, whilst in the latter suite enrichment in  $\delta^{18}\text{O}$  was also found in the marginal quartz diorites and in the small stock to the SE of the main complex. This enrichment is attributed to contamination by isotopically heavier metasedimentary rocks.

The most strongly hydrothermally altered rock types in the complex show an enrichment in  $\delta^{18}\text{O}$  and  $\delta\text{D}$ . Separate from alteration effects, there is a consistent pattern of enrichment of  $\delta^{18}\text{O}$  as function of differentiation index in the monzodiorite–quartz diorite suite, suggesting that the original oxygen isotopic composition of this suite was largely preserved. No systematic pattern was observed in the later granites, except for high values in the late leucogranite.

Eliminating samples in the vicinity of the contacts with the country rock metasediments, Hoernes *et al.* (1991) inferred that the  $\delta^{18}\text{O}$  values for the parental diorite

magma was in the relatively restricted range of +7.5 to +8.2‰, consistent with derivation from an igneous protolith in the lower crust or at the crust–mantle boundary. The higher  $\delta^{18}\text{O}$  values of the later granites may have been due either to a melt source richer in sedimentary material, or to contamination of the melts by greater amounts of  $^{18}\text{O}$ -enriched material of probable metasedimentary origin.

Contrasts in the  $\delta\text{D}$  and  $\delta^{18}\text{O}$  systematics of the monzodiorite–quartz diorite suite and the later granite suggests that there was little isotopic communication between the two magma batches, indicating that emplacement and crystallization of the later granites had little effect on the isotopic signature of the earlier diorites. This may have been due to the fact that the diorite shell was largely crystallized by the time the granite intruded, forming an impermeable barrier to outward fluid flow and favouring concentration of fluid toward the centre of the granite where secondary alteration is observed to be most intense.

Absolute values and mineral–mineral fractionations of  $\delta^{18}\text{O}$  and  $\delta\text{D}$  in magnetite, chlorite, titanite, biotite, hornblende and quartz do not indicate any significant late-stage, subsolidus exchange with meteoric fluids, and are considered to have been controlled by magmatic fluids (Hoernes *et al.* 1991). The stable isotope systematics of the igneous rocks, combined with the evidence of limited exchange of stable isotopes between igneous and aureole rocks (see below), suggest that the intrusion of the Ballachulish Complex did not lead to exchange with meteoric water or to the development of a large scale hydrothermal circulation system (Hoernes *et al.* 1991; Harte *et al.* 1991b).

#### Depth of emplacement and relation to the Glen Coe volcanic/plutonic centre

Pattison (1991, 1992) obtained a pressure estimate for the igneous complex and aureole of  $3.0 \pm 0.5$  kbar from several independent phase equilibrium techniques, all in excellent agreement. These included: a calibrated petrogenetic grid for metapelites in the aureole (Pattison 1989); calc–silicate equilibria (Masch and Heuss-Assbichler 1991); garnet–hypersthene–cordierite–plagioclase–quartz geobarometry (Pattison 1989); and comparative analysis of mineral compositions in the intrusive rock types with experimental phase equilibrium data (Weiss and Troll 1989). Assuming a lithostatic pressure gradient and an average density for overlying rocks of 2.7 g/cc, a pressure of  $3 \pm 0.5$  kbar corresponds to an emplacement depth of  $10 \pm 2$  km.

An emplacement depth of 10 km may appear somewhat high when it is considered that the broadly similar-aged (Siluro–Devonian) Glen Coe Complex, 10 km to the east, contains extrusive lavas. Age dating of the two complexes is not precise enough to establish a definitive age difference, and is complicated by the use of different techniques. Compared to the  $412 \pm 28$  Ma age for Ballachulish (combination of Rb–Sr and K–Ar dates; see compilation in Troll and Weiss 1991), Thirwall (1988) obtained an amphibole  $^{40}\text{Ar}$ – $^{39}\text{Ar}$  age of  $413$ – $421 \pm 15$  Ma for the Glen Coe lavas (his table 3). Some indication that the Ballachulish Complex is indeed older than the Glen Coe Complex is provided by a high precision titanite U–Pb age of  $427 \pm 3$  Ma

for the Rubha Mor intrusion of the Appinite suite (Rogers and Dunning 1991), which was emplaced immediately prior to, or contemporaneously with, the diorite phase of the Ballachulish Complex (Troll and Weiss 1991; see above). Bailey

and Maufe (1960) noted that the Glen Coe lavas must have subsided a considerable distance within the Glen Coe caldera complex, owing to the fact that the Leven Schists within the caldera are garnet-absent (i.e., relatively low grade) whereas Leven Schists outside the caldera are garnet-bearing (i.e., relatively higher grade). The subsidence reduces the apparent difference in emplacement level between the Ballachulish Complex and the Glen Coe lavas.

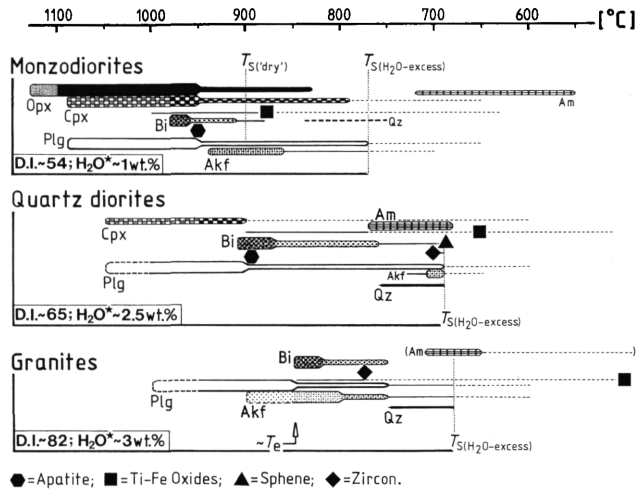


FIG. 5. Order of crystallization of minerals in the monzodiorites, quartz diorites and granites, with temperature estimates, based on methods described in Weiss (1986), Troll and Weiss (1991) and Weiss and Troll (1989, 1991). Assumed pressure is 3 kbar. D.I. = differentiation index.  $H_2O^*$  = water content of magma.  $T_s$  = solidus temperature.  $T_e$  = emplacement temperature. Sphene = titanite. The wider portions of each mineral pattern represent the main interval of crystallization; the narrower portions represent continued, but more minor, crystallization. Dashed margins (Plg, Akf) and fine stippled patterns (Opx, Cpx) at the high temperature end of each crystallization interval represent uncertainty in the temperature of initial crystallization.

### Summary of igneous emplacement and crystallization sequence

An emplacement history and crystallization sequence for the igneous complex was synthesized by Weiss and Troll (1989) and Troll and Weiss (1991) from their detailed thermometric and petrological-structural studies. Figure 5 shows the temperatures and inferred order of crystallization in the monzodiorites, quartz diorites and granites, based on textural evidence, pyroxene thermometry, and experimental stability data for pyroxenes, feldspars, biotite and amphiboles in melts of different compositions. Figure 6 shows a conceptual three-stage evolution of the igneous complex.

Initially, a relatively dry, alkaline, convecting monzodiorite magma with about 1 wt% water was emplaced in a largely liquid state at about 1100°C, forming a small elliptical stock measuring  $c. 3 \times 5 \text{ km}^2$  (Stage I, Fig. 6a). Hyperssthene, augite and andesine initially crystallized in the interval 1100–950°C, followed by Fe–Ti oxides (1000–880°C), biotite (980–910°C), apatite ( $c. 950^\circ\text{C}$ ) and alkali feldspar (940–860°C). During crystallization of hyperssthene, augite and andesine, a cylindrical, sub-vertical crystal mush zone slowly advanced from the outer contacts towards

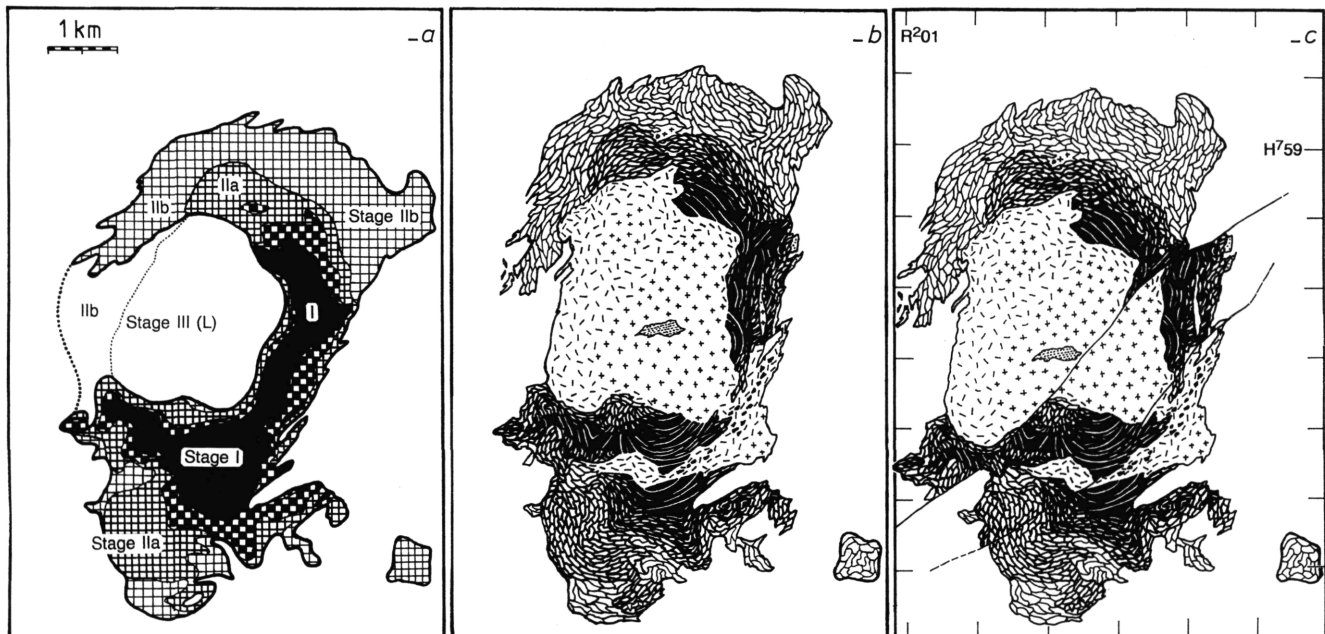


FIG. 6. Conceptual evolution of the Ballachulish Igneous Complex, from Weiss (1986) and Troll and Weiss (1991). (a) Stages in the permissive emplacement and fractionation of the diorite magmas. (b) Forceful intrusion of granite magma into the partially consolidated diorites. (c) Final configuration of the Igneous Complex after post-intrusion faulting. *Black*, Opx-Cpx monzodiorite. *Check*, Opx-Cpx quartz diorite. *Fine cross-hatch*, Cpx-Amph quartz diorite. *Medium cross hatch*, Bt-Amph quartz diorite. *Crosses* – granite. *Random short lines* – transitional granite. *Stippled area in centre of granite* – leucogranite. In b and c the ornaments are modified to show schematically the igneous lamination and deformation foliation of the diorites.



pelitic rocks (Pattison 1985, 1987, 1989, 1991, 1992; Pattison and Harte 1985, 1988, 1991; Harte *et al.* 1991a). Five metamorphic zones can be mapped, based on the distribution of the minerals: muscovite (Ms), quartz (Qtz), chlorite (Chl), biotite (Bt), cordierite (Crd), K-feldspar (Kfs), andalusite (And), sillimanite (Sil), corundum (Crn), garnet (Grt), spinel (Spl) and hypersthene (Hy) (abbreviations from Kretz 1983). Zones I–IV contain the stable subassemblage Ms + Qtz, whereas Zone V contains the stable subassemblage  $Al_2SiO_5$  + Kfs. Simplified model reactions, consistent with modal and chemical variations, have been written for each isograd (see Pattison and Harte 1991 for more detail). Most of these reactions and their estimated temperatures are indicated on Figure 3, and they are given the prefix 'P' (for pelite) to distinguish them from carbonate reactions discussed below.

Figure 7 shows a calibrated petrogenetic grid in  $P$ – $T$  space (for  $P_{H_2O} = P_{rock}$ ) that accounts for the prograde assemblage sequence in quartz-bearing rocks. Figure 8 shows a schematic isobaric  $T$ – $X_{Fe-Mg}$  diagram showing the

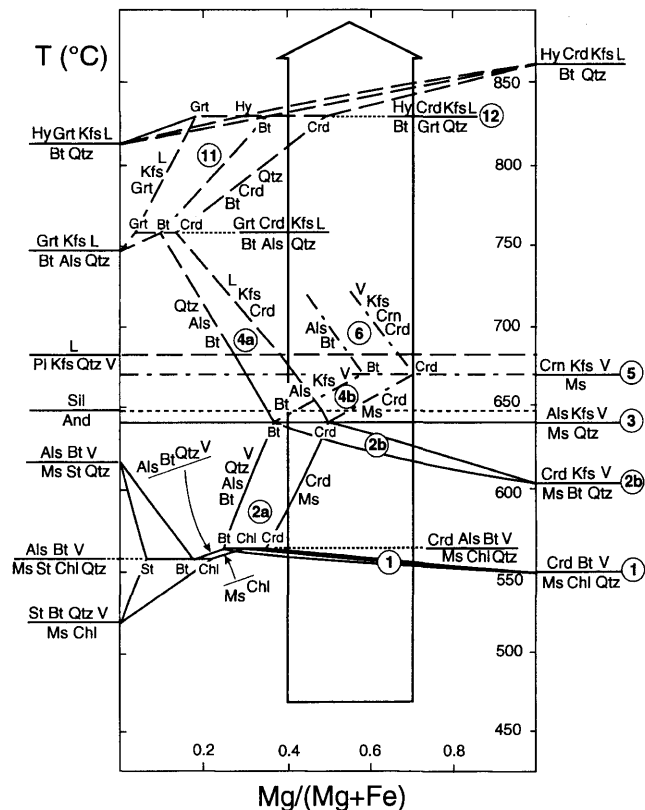


FIG. 8. Semi-quantitative 3 kbar  $T$ – $X_{Fe-Mg}$  diagram, modified from Pattison (1989) and Pattison and Tracy (1991). Solid lines are for quartz-bearing reactions; dash-dot lines are for quartz-absent reactions; dashed lines are for the melting reactions; and short-dashed line is the andalusite-sillimanite transition. Dotted lines allow the arrangement of reactants and products to be shown for the isobarically invariant reactions (univariant reactions in Fig. 7). For clarity, reaction (P6) has not been extended up-temperature to intersect with numerous quartz-absent reactions involving spinel, garnet and hypersthene (see Pattison and Harte 1991, for further details). The broad arrow represents the majority of natural compositions in the aureole. *Als*, andalusite and/or sillimanite. *V*, hydrous vapour, *L*, silicate melt.

effect of Fe/Mg ratios on the stabilities of quartz-bearing and quartz-absent assemblages. Temperature ranges for the different isograds (legend of Fig. 3 and below) take account of measured compositional variations, principally Fe–Mg and presence or absence of graphite, the latter which affects the assumption of  $P_{H_2O} = P_{rock}$  (see Pattison 1989 for details and for discussion of uncertainties). The assumption of an isobaric  $P$ – $T$  trajectory is supported by thermal modelling of the contact metamorphic event: even assuming the fastest rates of uplift ( $0.5 \text{ mm/a}^{-1}$ ; Dempster 1985) estimated for the Dalradian between 410 and 390 Ma (approximately the time of emplacement of the Ballachulish intrusion), the amount of uplift between the time of intrusion and establishment of the cordierite isograd (c. 0.2 Ma) will have been only 100 m (c. 0.03 kbar).

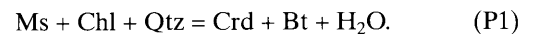
### Zone I (Marginal zones)

Zone I comprises regional grade schists that show no obvious contact metamorphic effects. The two main regional grade assemblages are Ms + Chl + Qtz ± Bt and Ms + Chl + Qtz + Bt + Grt, depending on position and lithology with respect to the garnet isograd (see Fig. 1 and section on regional metamorphism).

### Zones II and III (Lower cordierite zones)

The lower cordierite zones comprise spotted slates and phyllites, with the spots representing contact metamorphic cordierite. Two zones of increasing grade are recognized: Zone II, the chlorite zone, containing the assemblage Ms + Chl + Qtz + Crd + Bt, and Zone III, the chlorite-absent zone, containing the assemblage Ms + Qtz + Crd + Bt.

Zone II is less than 200 m wide (typically < 100 m) and can only be mapped as a separate zone in certain parts of the aureole (Fig. 3). Incipient cordierite in Zone II occurs as minute, ca. 1 mm wide ellipsoidal spots on cleavage and bedding surfaces in phyllitic rocks, and is accompanied by biotite (not usually visible in outcrop). A short distance upgrade of the first appearance of cordierite (spotting), the rocks become less fissile, the modal abundance and grain size of cordierite increases markedly and the modal abundance of chlorite decreases. The model reaction (550–560°C) that accounts for the production of cordierite and biotite at the expense of chlorite is:

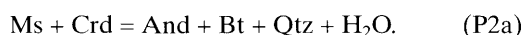


Zone III contains the same assemblage as Zone II except that primary chlorite is no longer part of the assemblage, having been consumed in the production of cordierite and biotite through reaction (P1). Zone III is the widest single metamorphic zone in the aureole (Fig. 3). Spotted phyllites and slates of Zone III are more massive and recrystallized than those of Zone II, and become increasingly hornfels-like as grade increases. Regional grade garnet is replaced and pseudomorphed by cordierite and biotite in Zone III.

### Zone IV (Upper cordierite zones)

Upgrade of Zone III, metapelites acquire either of the assemblages And + Crd + Bt + Ms + Qtz (assemblage IVa) or Kfs + Crd + Bt + Ms + Qtz (assemblage IVb). These assemblages are developed in rocks of different bulk composition at the same grade. Assemblage IVa has only been observed in the graphite-rich Ballachulish Slate and Transition Series lithologies in the southeast part of the aureole, whereas assemblage IVb is found in all other stratigraphic units, and hence is the more common of the two assemblages (Fig. 3).

*Assemblage IVa.* Upgrade of Zone III in the Ballachulish Slate and Transition Series, andalusite joins the Ms + Crd + Bt + Qtz assemblage, typically occurring either in tiny (*c.* 1 mm), ill-formed crystals that produce a rough texture on weathered surfaces, and more rarely in elongate (up to 5 mm long) prisms visible on cleavage surfaces. In thin section, andalusite tends to occur in ragged crystals adjacent to cordierite and is typically intergrown with biotite and quartz. The model reaction (*c.* 600°C) consistent with the modal changes and textures is:



*Assemblage IVb.* In all units other than the Ballachulish Slate and Transition Series, K-feldspar joins the Ms + Crd + Bt + Qtz assemblage upgrade of Zone III. The development of K-feldspar coincides with a relatively abrupt textural transition from spotted phyllites and slates to massive hornfelses, due to a combination of an increase in cordierite abundance and the development of K-feldspar. The K-feldspar typically occurs in the matrix of the hornfels around the margins of the cordierite poikiloblasts, producing a distinctive white ribbed network of upward-weathering K-feldspar-rich material surrounding ovoid depressions left by weathered cordierite. Primary muscovite decreases markedly with grade in this zone, and disappears entirely in semipelitic layers, giving the common assemblage Bt + Crd + Kfs + Qtz. An approximate muscovite-out isograd in semipelites has been mapped in the Coire Giubhsachain syncline on the NE flank of the complex. The model reaction (*c.* 620°C) accounting for the production of K-feldspar and cordierite and the consumption of muscovite is:



*Controls on the development of Assemblages IVa and IVb.* The relative development of assemblage IVa and IVb is affected by both Fe-Mg ratio and volatile composition (Pattison 1987, 1989, 1991). Referring to Fig. 8, andalusite-bearing assemblage IVa occurs in the reaction P2a field and is favoured in more Fe-rich compositions, whereas K-feldspar-bearing assemblage IVb (reaction 2b field) is favoured in more Mg-rich compositions. Measured mineral compositions, however, show overlap in Fe-Mg between the two assemblages, and suggest that the two

assemblages formed under different fluid compositions. This has been shown to be linked to the presence of graphite in the Ballachulish Slate and Transition Series, making the fluid composition in these lithologies more water-poor and causing the preferential expansion of the stability field of assemblage IVa relative to assemblage IVb (Pattison 1989, 1991).

### Zone V (Al<sub>2</sub>SiO<sub>5</sub> + K-feldspar zone).

The boundary between Zones IV and V is marked by the first appearance of andalusite + K-feldspar and the abrupt decrease of primary muscovite or quartz. Sillimanite makes its first appearance at about the same grade as the first appearance of And + Kfs. The model reaction (625–640°C, depending on the presence or absence of graphite) that accounts for the abrupt appearance of And + Kfs and the disappearance of coexisting quartz and primary muscovite is:



Hornfelses within Zone V can be divided into quartz-bearing, primary muscovite-absent varieties or muscovite-bearing, quartz-absent varieties. Separate prograde sequences of assemblages are developed in each bulk composition. Up to the onset of partial melting, quartz-bearing assemblages maintain a common assemblage, whereas in quartz-absent hornfelses, a lower grade subzone Va (muscovite subzone) and higher grade subzone Vb (corundum subzone) may be distinguished.

*Andalusite and sillimanite.* Andalusite is by far the most common Al<sub>2</sub>SiO<sub>5</sub> mineral in Zone V and is the only one visible in hand specimen. It occurs in prominent elongate 2–5 mm long euhedral–subhedral prisms, associated with K-feldspar, quartz and sometimes biotite. Sillimanite first occurs sporadically in assemblages in the low grade part of Zone V (Pattison 1992) and, when present, is always fine-grained and in small modal abundance (Sil/(And + Sil) < 1%). The abundance and grain size of sillimanite generally increases upgrade in Zone V, although even in the highest grade hornfelses, andalusite is typically more abundant (Pattison 1992). Some rocks well upgrade of the first appearance of sillimanite contain andalusite with no sillimanite, thereby demonstrating the sluggishness of the polymorphic inversion reaction and the importance of kinetic factors to the development of sillimanite. For these reasons, a sillimanite isograd has not been mapped, although its lowest grade occurrence is either coincident with or very slightly (< 50 m) upgrade of the first appearance of And + Kfs (P3 isograd at the start of Zone V in Fig. 3).

*Quartz-bearing assemblages of Zone V.* The majority of quartz-bearing hornfelses in Zone V contain the assemblages Bt + Crd + Kfs + Qtz and And(Sil) + Bt + Crd + Kfs + Qtz, both of which persist up to the igneous contacts. The first assemblage may have been formed at lower grade by reaction (P2b), and persisted unaffected through reaction (P3) due to the absence of muscovite. The second

assemblage most likely developed when muscovite was consumed by reaction (P3). The minerals of the second assemblage are related by the following model reaction:



*Quartz-absent assemblages; Subzone Va (Muscovite subzone).* Subzone Va, the muscovite subzone, is defined by the quartz-absent assemblage  $\text{Ms} + \text{Crd} + \text{Bt} + \text{And}(\text{Sil}) + \text{Kfs}$ . This zone has only been mapped in the Coire Giubhsachain syncline on the NE flank of the complex, where appropriate lithologies are sufficiently abundant. The minerals of the assemblage are related by the following model reaction:



*Quartz-absent assemblages; Subzone Vb (Corundum subzone).* The appearance of corundum in quartz-absent assemblages marks the lower boundary of subzone Vb, the corundum subzone. Corundum occurs in small, 1–2 mm, rounded grains that weather up on outcrop surfaces, and contrast with the larger, more prismatic andalusite crystals which typically occur in the same rocks. The model reaction (650–670°C) accounting for the initial development of corundum is:



At higher grades in Zone Vb, the most common assemblage is  $\text{Bt} + \text{Crd} + \text{And}(\text{Sil}) + \text{Crn} + \text{Kfs}$ , which persists well into the migmatite subzone. The assemblage is involved in the model reaction:



#### Cordierite distortion index

Maresch *et al.* (1991) conducted a study on the structural state of cordierite in the aureole, and found a minor trend in the distortion index as a function of distance from the igneous contact. All values were indicative of low (ordered) orthorhombic cordierite ( $\Delta = 0.23\text{--}0.30$ ), with higher  $\Delta$  values occurring nearer the igneous contact. From petrological considerations, Pattison (1989) and Maresch *et al.* (1991) argued that cordierite nucleated and grew in its orthorhombic, low-temperature form and never went through a disordered, hexagonal stage as suggested by Schreyer (1966) and Putnis and Holland (1986).

#### Anatectic migmatization

In the upper part of Zone V, within 400 m of the igneous contact but most typically within 100 m of the contact, a range of structures and textures in pelitic and semipelitic lithologies are suggestive of the localized occurrence of partial melting (Pattison and Harte 1988; Harte *et al.* 1991a). The rocks concerned can be described as migmatites because they contain leucocratic domains (leucosomes) in association with mesosomes and selvages that might be termed melanosomes (terminology of Ashworth 1985).

In contrast to the subsolidus isograds, the partial melting 'isograd' does not involve any abrupt modal mineralogical changes, being characterized instead by a range of outcrop structures and hand specimen/thin section textures. Several different types of structures associated with melt generation may be seen in the aureole and the more prominent of these are summarised below (see Harte *et al.* 1991a for a detailed treatment, and Pattison and Harte 1988 and Harte *et al.* 1991a for photographs).

*Pull-apart and breccia-like migmatites.* These melt-related structures are typically formed in metasedimentary rocks showing well developed pre-existing layers or laminae which represent original bedding structures. They involve the millimetre–centimetre scale pull-apart of cordierite-rich and psammitic layers and the infilling of the volume between the resulting dismembered boudin-like fragments by apparently mobile material, which varies from being distinctly leucocratic (Kfs and/or Qtz-rich, with minor biotite, plagioclase and tourmaline) with granitic- to micro-pegmatitic textures, to material with more biotite and a more semipelitic appearance. In some rocks in which pulled-apart cordierite-rich layers are interlayered with semipelite, the semipelite shows evidence for flow or bending towards the gaps between the pulled-apart fragments. The centres of the gaps are typically filled with the granitic material, which grades continuously into the semipelite and hence appears to have been extracted from the semipelite. The brittle hornfels layers/fragments are typically cordierite-rich and quartz-poor; but thin quartzite and calc-silicate layers may behave in the same brittle fashion.

In many cases the orientation of the original layering is largely preserved, and whilst leucosomes both crosscut and occur parallel to the layering, they generally show restricted continuity across the layering (i.e., they are not through-going like normal vein structures). More extensive mobility of leucosome results in break-up and disorganization of hornfels and psammitic layers, leading to the formation of breccia or agmatitic structures in which fragments of hornfels with irregular orientations are suspended ('floating') in quartzofeldspathic leucocratic material.

The above structures are accompanied by a range of thin-section scale textures typically found in granites and pegmatites which further imply the former presence of melt, including: coarse grained, quartz-cored quartzofeldspathic segregations resembling zoned pegmatites; granophyric intergrowths of quartz and K-feldspar; quartz showing interstitial textures between feldspar, cordierite, biotite and andalusite; euhedral-subhedral cordierite and perthitic K-feldspar crystals; intergranular albite rims around K-feldspar crystals; and late, coarse-grained poikilitic biotite. The above features, combined with the presence of sedimentary isotope signatures (Linklater 1990; Linklater *et al.* 1994), suggest that the melt represented by the leucosomes was generated *in situ* within the metasediments.

Development of melt resulted in some layers becoming relatively ductile. The brittle fracturing and pulling apart of the hornfels and other layers was accompanied by flow of the ductile, melt-bearing semipelitic material, with the granitic-type leucosome being extracted from the

melt-bearing semipelite. The flow of the semipelitic material suggests that the critical melt fraction (the volume fraction of melt required for a mixture of solid particles plus melt to behave as a fluid-supported suspension, *c.* 30–40% melt; Van der Molen and Paterson 1979) was locally exceeded in these layers. The extensional fracturing process represented by the boudinage and breccia structures may have been due to volume increases resulting from melting (see below): the increased fluid (melt) pressure reduced effective stresses such that the least principal compressive stress became tensional, leading to hydraulic fracturing. Pull-apart migmatites are seen locally all around the igneous contacts, but are best developed in: the Coire Giubhsachain syncline on the NE of the complex; west of Sgorr Dhearg in a country rock screen within the igneous complex; in the SE above Coire Chaorainn; and locally near Kentallen.

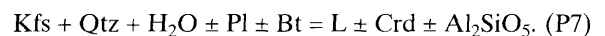
*The Chaotic Zone.* This zone, on the west flank of the igneous complex, is characterized by disruption of layering on a much more extensive scale than elsewhere in the aureole. Two main rock types occur: obvious metasedimentary rock, including layered varieties and cordierite- and andalusite-rich hornfelses like those described in the pull-apart migmatites; and relatively homogeneous rock with a granular appearance, resembling quartzofeldspathic-rich semipelitic rock. The first rock type typically occurs as diversely orientated fragments suspended in or surrounded by the more granular semipelitic rock. A diffuse foliated structure may be present in the granular rock, sometimes bending in a manner suggestive of flow. The proportion of the rock types varies considerably, giving rise to all gradations between agmatitic migmatites, in which there are a large number of variably orientated fragments in the granular semipelite, and schollen migmatites, in which relatively few, isolated fragments (xenoliths) occur in the granular semipelitic matrix. Granitic- and pegmatitic-type leucosomes, such as those found in between fragments in the pull-apart migmatites, are generally absent. Locally, dykes of granite and granodiorite of the igneous complex sharply cross-cut both the granular semipelite and rigid fragments, suggesting that the mobility of the semipelitic material was due to internal melt generation rather than mixing with magmatic material from the igneous complex, a view supported by isotope studies of these rocks (Linklater *et al.* 1994).

The greater extent of disruption in the Chaotic Zone migmatites compared with migmatites elsewhere in the aureole is attributed to larger degrees of partial melting coupled with their more homogeneous semipelitic composition. The granular semipelitic matrix to the rigid metasedimentary fragments appears to have undergone bulk flow as a suspension of crystals in melt, suggesting that the critical melt fraction was exceeded in a considerable portion of the rock mass in this zone. In contrast to the pull-apart migmatites found in more heterogeneous rocks elsewhere in the aureole, melt may have been retained in the semipelitic rock in which it was generated, rather than separating from crystals and migrating into leucocratic segregations, owing to fewer appropriate sites

(*e.g.*, gaps between brittle layers) for separation. The disruption of layering and evidence for flow in the Chaotic Zone migmatites may have been caused by the emplacement and ballooning of the immediately adjacent central granite when the migmatites were still molten.

The greater degree of melting in the Chaotic Zone compared to other parts of the aureole is most likely related to the occurrence of quartz diorite at relatively shallow depths beneath this zone. Pattison and Harte (1988) and Weiss and Troll (1989) estimated that the solidus of the semipelitic rocks of the Chaotic Zone (660–680°C) was lower than that of the underlying quartz diorite (680–700°C). Migration of hot aqueous magmatic fluids from the crystallizing diorite upwards into the overlying hot metasediments may therefore have caused the large degrees of partial melting (see discussion below). Linklater *et al.* (1994) showed that a relatively small transfer of fluid could have significantly affected melt production.

*Melting reactions and the importance of water influx.* The onset of partial melting at Ballachulish is interpreted to be due to water-consuming reactions of the form:



This reaction emphasizes the essential participation of quartz, K-feldspar and water to produce the Kfs + Qtz-rich leucosomes, and the selective participation of the other minerals, depending on the exact composition of the protolith. The temperature for initiation of water-consuming melting in non-graphitic rocks is 660–680°C (Pattison 1991). Initial partial melting by reaction (P7) requires free H<sub>2</sub>O as a reactant to proceed: in the absence of water, no partial melting due to reaction P7 may occur, whereas if water is introduced to the site of melting, extensive melting may occur at relatively modest (*e.g.*, < 700°C) temperatures. Rocks hot enough to undergo partial melting will therefore have provided a barrier to the flow of hydrous fluid in the aureole because the H<sub>2</sub>O will have been consumed to generate melt.

Within the Ballachulish aureole both types of fluid-controlled behaviour are seen. Large volumes of quartzofeldspathic semipelitic rocks on the east and south flanks show little evidence for migmatization, even though mineral assemblage constraints and thermal modelling indicate that temperatures (> 700°C) were well above the minimum required for melting by reaction P7. In these rocks, lack of melting was probably due to lack of introduced water, consistent with the evidence of generally restricted fluid movement in the aureole (Harte *et al.* 1991*b*). By contrast, in the Chaotic Zone, partial melting was extensive even though the metamorphic temperatures in the Chaotic Zone (rare sillimanite; no spinel, garnet or hypersthene; stable calcite + chlorite-bearing assemblages in immediately adjacent calcisilicates) were lower (< 700°C) than many other parts of the aureole that show little evidence for migmatization (*e.g.*, south and east flanks). We believe it was the availability of H<sub>2</sub>O from the underlying quartz diorite which enabled the extensive melting of the Chaotic Zone.

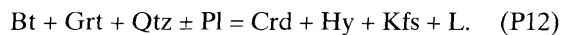
### High-grade mineral assemblages

Some particularly high-grade mineral assemblages occur sporadically within the subzone of partial melting, and are shown on Figure 3 as lettered localities. In quartz-bearing rocks adjacent to the southern contact and in an isolated metasedimentary screen west of Sgorr Dhearg (localities marked G on Fig. 3), red 1-3 mm garnets occur in the assemblage Bt + Crd + Grt + Qtz + Kfs + Pl + Ilm. In the large metasedimentary raft in the quartz diorite near the SE contact, orthopyroxene (hypersthene) joins the above assemblage, giving rise to a low pressure granulite facies assemblage (locality marked GO, Fig.3). The hypersthene-bearing rocks are the highest grade rocks in the aureole.

The model reactions accounting for the production of garnet and hypersthene in the above assemblages are, respectively:



and



In contrast to reaction (P7), these reactions are water-conserving 'dehydration melting' reactions (Thompson 1982), in which the H<sub>2</sub>O that enters the melt phase is supplied by the decomposition of biotite rather than from a free fluid phase. Reactions (P11) and (P12) occur in the temperature interval 810–850°C at 3 kbar (Vielzeuf and Montel 1994; Carrington and Harley 1995), somewhat higher than the 750–800°C estimate of Pattison (1991) from geothermometry. Migmatitic features in the high grade Grt- and Hy-bearing rocks may be due in part to melt production that accompanied generation of garnet and hypersthene.

In quartz-absent rocks in the subzone of partial melting, pleonaste spinel is present in the assemblage Spl + Crd + Crn + Bt + Ilm ± Al<sub>2</sub>SiO<sub>5</sub> ± Pl (localities marked 'S' in Fig. 3). The model reaction accounting for the production of spinel is:



Because the solidus for quartz-absent rocks is considerably higher than for quartz-bearing rocks, this reaction and reaction (P6) may have been subsolidus dehydration reactions rather than dehydration melting reactions. Water released from reactions (P6) and (P8) in quartz-absent, cordierite-rich layers in the pull-apart type of migmatites might have helped flux the melting in the adjacent ductile, quartzofeldspathic semipelitic layers (Pattison and Harte 1988).

### Contact metamorphism of siliceous carbonates

Siliceous carbonates are widespread as thin layers in various parts of the aureole, but nowhere is it possible to follow a single unit continuously from outside the aureole to the igneous contact. The best exposure is in the Coire Giubhsachain syncline on the NE flank of the igneous complex, where siliceous carbonates can be traced from middle-grade conditions up to the igneous contact (Zones III-V in interbedded pelites).

Two sets of studies have been concerned with the phase equilibria in the siliceous carbonates: Masch and

Heuss-Assbichler (1991) and Heuss-Assbichler and Masch (1991) on the one hand, and Ferry (1996a, b) on the other. Masch and Heuss-Assbichler's studies were principally concerned with the prograde mineral assemblages and petrogenesis, whereas Ferry's studies concentrated on both the prograde and retrograde minerals and petrogenesis. The section below focuses mainly on the prograde mineral assemblages and isograds.

The siliceous carbonates can be divided into two main types: siliceous dolomites and impure limestones. Outside the aureole, the typical assemblage of siliceous dolomites is dolomite (Dol) + calcite (Cal) + Qtz, with variable amounts of Chl, Ms, Bt, and pyrite. In impure limestones the regional assemblage has more Cal, but contains the same phyllosilicates as in the siliceous dolomites with the addition of albite, microcline and pyrite. Owing to the generally fine grain size of the siliceous carbonates in the aureole, index minerals are not easily identified in outcrop and have been identified mainly using the optical microscope and scanning electron microscope (exceptions are the coarse grained garnet-bearing calcsilicates discussed below).

Figure 9 shows a map of isograds in the mid-high grade rocks in the Coire Giubhsachain syncline. Model reactions corresponding to the isograds follow the same numbering scheme in the isobaric  $T$ - $X_{\text{CO}_2}$  diagram of Figure 10. Most of the isograds are related to isobarically univariant reactions in the model system CaO-MgO-SiO<sub>2</sub>-H<sub>2</sub>O-CO<sub>2</sub> (CMSh-CO<sub>2</sub>), which Masch and Heuss-Assbichler (1991) showed is a good model system for first-order analysis of the phase equilibria (although deviations from this system are important in temperature estimation; Ferry, 1996a, b). Some additional equilibria involving grossular garnet and spinel in the system Al<sub>2</sub>O<sub>3</sub>-CMSh-CO<sub>2</sub> were calculated using the thermodynamic data base of Berman (1988; unpublished 1993 update) and plotted on Figure 10. Temperatures for the different isograds are based on calcite-dolomite geothermometry and from calcsilicate phase equilibrium constraints (Masch and Heuss-Assbichler 1991; Ferry 1996a). Ferry (1996a) concluded that several of the calcite-dolomite temperatures from Masch and Heuss-Assbichler (1991) are rather low and may reflect resetting.

### Carbonate and calcsilicate isograds

*Distribution of talc.* On the edge of the aureole talc occurs in the assemblage Tlc + Cal + Dol + Qtz in siliceous dolomites 200–300 m outside the cordierite-in (P1) isograd. Talc in the assemblage Tlc + Mgs + Qtz occurs in magnesite-bearing rocks 200–300 m downgrade of talc in siliceous dolomites in the SE (Masch and Heuss-Assbichler 1991). The limited distribution of these assemblages makes it difficult to assess their contact and regional metamorphic relationships. However, their spatial distribution around the edge of the aureole, and the fact that Tlc + Mgs assemblage occurs downgrade of the Tlc + Dol assemblage, consistent with calculated phase equilibria (reactions C1 and C1' in Fig. 10), may suggest a contact metamorphic origin.

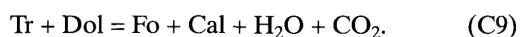
*Diopside isograd in impure limestones.* An isograd (C6) marking the incoming of diopside in impure limestones (assemblage diopside (Di) + tremolite (Tr) + Qtz + Cal) has been mapped by Masch and Heuss-Assbichler (1991) on the eastern edge of the Allt Giubhsachain syncline (Fig. 9). The reaction inferred to have produced diopside is:



The lack of exposures of Di-free assemblages downgrade of the indicated isograd means that the isograd could lie at greater distances from the igneous contact. Calcite–dolomite thermometry from one sample containing the reaction assemblage yields 520°C, whereas the maximum temperature according to Figure 10 is 570°C.

*Forsterite + diopside + tremolite + calcite + dolomite assemblages and related isograds.* In quartz-absent siliceous dolomites, combinations of Cal, Dol, Di, Tr and forsterite (Fo) occur over an approximately 250 m wide zone upgrade of isograd C6 in impure limestones. Masch and Heuss-Assbichler (1991) mapped a series of isograds corresponding to isobarically univariant subsets of these minerals (Fig. 9). Ferry (1996b) re-investigated the assemblages in this zone, and concluded that the full five phase assemblage was more widespread than found by Masch and Heuss-Assbichler (1991). In the ensuing discussion, we describe first the isograds as interpreted by Masch and Heuss-Assbichler (1991), and then discuss Ferry's interpretation.

*Forsterite + calcite isograd.* Masch and Heuss-Assbichler (1991) found that Tr + Dol assemblages in siliceous dolomites passed upgrade into Tr + Dol + Cal + Fo assemblages. They took the first appearance of Fo + Cal to mark the Fo + Cal isograd (9 on Figs. 9 and 10), represented by the following model reaction:



Calcite–dolomite thermometry from a sample near the isograd yielded about 530°C, whereas the maximum temperature possible is about 620°C (see Fig. 10). The latter temperature is more consistent with the location of the isograd within Zone IVb (620–640°C) of the interbedded pelitic rocks.

*Diopside + forsterite isograd.* Masch and Heuss-Assbichler (1991) found that Di + Fo assemblages appeared upgrade of Tr + Cal assemblages, slightly upgrade of the Fo + Cal isograd. The inferred reaction is:



Temperature constraints for this isograd are very similar to those for the Fo + Cal isograd.

*Diopside + forsterite + tremolite + calcite + dolomite isograd.* About 200 m upgrade of the C9 and C10 isograds, Masch and Heuss-Assbichler (1991) found the five phase

assemblage Di + Fo + Tr + Cal + Dol in several samples over a 100 m interval (Fig. 9). Assuming all five phases were in equilibrium, they interpreted these assemblages to represent an isobaric invariant assemblage in the model CMSH–CO<sub>2</sub> system (CIII; Fig. 10). This assemblage records 620°C, in excellent agreement with calcite–dolomite thermometry of 620°C and with the 625–640°C estimate from the nearby And + Kfs isograd in metapelites.

Masch and Heuss-Assbichler (1991) found that some samples of the five-phase assemblage show textural evidence of arrested replacement of Cal + Tr by Di + Dol, and of diopside by Fo + Cal. They interpreted these features to indicate progress of reactions C7 and C11 which emanate from the CIII invariant point in Fig. 10.

*Interpretation of Fo+Di+Tr+Cal+Dol assemblages by Ferry (1996b).* Using backscattered electron imaging, Ferry (1996b) found that tremolite was more widespread in the rocks than indicated by Masch and Heuss-Assbichler (1991). He distinguished between prograde ('peak') tremolite and retrograde tremolite based on texture and chemical criteria, and found that both prograde and retrograde tremolite occurs in the interval upgrade of isograds C9 and C10, and as far as isograd C11. He attributed the occurrence of the model isobaric assemblage over a fairly wide interval to deviations from the model end member composition of tremolite, which his calculations showed could be reconciled with the thermal gradient over this interval. The only isograd he could map in this interval was the diopside-out isograd (C11 in Fig. 9).

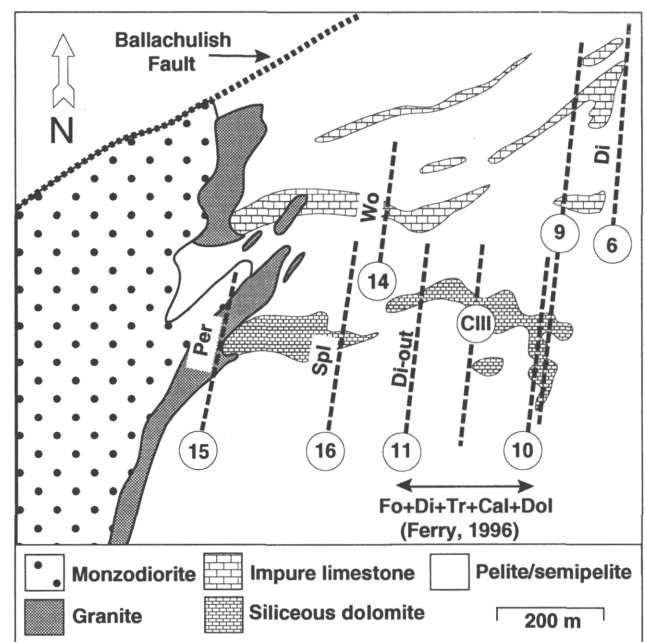


FIG. 9. Isograds in carbonate rocks from the Coire Giubhsachain syncline, northeast flank of igneous complex, compiled from Pattison (1985), Heuss-Assbichler (1987), Masch and Heuss-Assbichler (1991) and Ferry (1996b). Numbering of isograds is the same as in the text (with 'C' prefix omitted). Circled numbers and symbols 9, 10, CIII, 15 and 16 refer to assemblages and isograds observed in siliceous dolomites, whereas circled numbers 6, 9 and 14 are for isograds in impure limestone.

**Wollastonite isograd.** In impure limestones, the first appearance of wollastonite marks the wollastonite isograd, inferred to be due to the model reaction:



The first appearance of wollastonite in Coire Guibhsachain (Fig. 9) coincides approximately with the corundum and partial melting isograds in interbedded pelitic rocks, indicating a temperature of about 670°C for this isograd.

**Periclase isograd.** The highest grade mineral assemblages in impure dolomites contain periclase (Per). In only one sample has fresh periclase been found, with the rest containing brucite inferred to have replaced periclase.

These assemblages are restricted to dolomite xenoliths and/or screens within the marginal granite on the north-east flank of the igneous complex (Fig. 9), and in isolated outcrops within 200 m of the contact in the Kentallen area.

The inferred reaction for the production of periclase is:



Calcite–dolomite thermometry indicates a temperature of 760°C for these assemblages.

**Spinel isograd.** Although not mapped as an isograd by Masch and Heuss-Assbichler (1991) or Ferry (1996b), spinel occurs sporadically in high grade Fo + Cal + Dol ± Per-bearing siliceous dolomites, first occurring around or slightly upgrate of the wollastonite isograd. A spinel isograd (16) has been added to Figure 9 based on these occurrences, but its location is not tightly constrained. The most likely reaction accounting for the formation of spinel in these assemblages, consistent with the occurrence of chlorite in some lower grade marbles, is:



A minimum temperature for Spl + Fo + Cal + Dol assemblages (reaction (16) in Fig. 10) is about 650°C.

**Assemblages in calc-silicates.** Adjacent to the igneous contact along the ridge west of Coire Guibhsachain, layered calc-silicate rocks formed from impure limestones occur interleaved with semipelitic rocks and marbles and contain a wide range of mineral assemblages. Particularly striking are massive sheets, sometimes complexly folded, of medium-coarse grained rocks rich in grossular ± vesuvianite ± epidote, with variable amounts of calcite, amphibole, clinopyroxene, prehnite, wollastonite, scapolite, chlorite, muscovite, biotite, K-feldspar and plagioclase, plus numerous accessory phases. Many of the phases may not co-exist in stable equilibrium, some possibly having formed during later alteration processes. The grossular garnet contains up to 40% andradite component. Preliminary temperature estimates for Gr + Pl + Wo ± Cal ± Qtz calc-silicates about 150 m from the contact are around 650–700°C (Pattison 1985), consistent with estimates from adjacent siliceous carbonate and pelitic rocks. Conspicuous grossular-bearing marbles occur in isolated screens in the contact zone west of Sgorr Dhearg.

On the west flank of the igneous complex, layered grossular- and vesuvianite-bearing calc-silicates are found south of Kentallen. Immediately west of the disrupted migmatites of the Chaotic Zone, marbles contain combinations of calcite, dolomite, forsterite, diopside, phlogopite and rarely wollastonite and spinel, whereas calc-silicate rocks contain combinations of calcite, dolomite, quartz, plagioclase, diopside, tremolitic amphibole, epidote, biotite and chlorite. The apparently stable association of chlorite and calcite and absence of spinel in some layers limits the temperature to less than about 670 °C in this vicinity (reaction C(17) in Fig. 10).

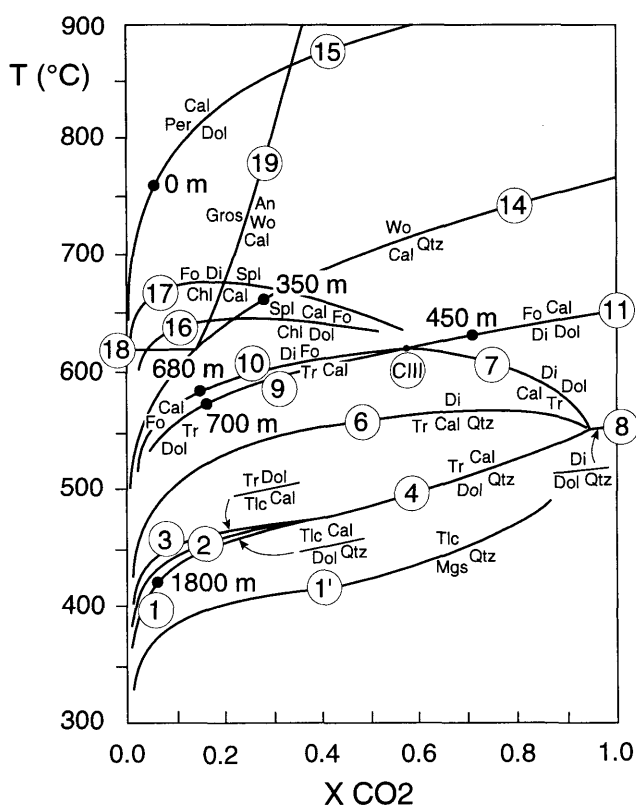


FIG. 10. Isobaric  $T$ - $X_{\text{CO}_2}$  diagram (3 kbar) for selected equilibria in the chemical system  $\text{CaO-MgO-SiO}_2\text{-Al}_2\text{O}_3\text{-H}_2\text{O-CO}_2$ , showing numbered reactions discussed in the text (modified from Masch and Heuss-Assbichler 1991).  $T$ - $X_{\text{CO}_2}$  positions of individual assemblages (small circles) are from intersections of temperature estimates along profile A in Figure 3 with the appropriate reaction (Masch and Heuss-Assbichler 1991); distances for these assemblages are from an averaged position of the monzodiorite contact in Figure 9, eliminating wiggles, as shown in Fig. 13 of Heuss-Assbichler (1987). Calculated positions of reactions C(1)-(15) are from Masch and Heuss-Assbichler (1991); reactions C(16)-(19) were calculated using thermodynamic data of Berman (1988, 1993 update). All reactions except C(18) involve  $\text{H}_2\text{O}$  and/or  $\text{CO}_2$ . Unlabelled reactions are as follows (phases on the right hand side of the reactions are on the high-temperature side):  
2.  $\text{Tlc} + \text{Cal} + \text{Qtz} = \text{Tr} + \text{CO}_2 + \text{H}_2\text{O}$   
18.  $\text{Gros} + \text{Qtz} = \text{An} + \text{Wo}$ .

*Isograds involving accessory minerals.* Ferry (1996a) documented the occurrence of three unusual isograds in Coire Guibhsachain involving the accessory phases rutile ( $\text{TiO}_2$ ), geikielite ( $\text{MgTiO}_3$ ), qandilite ( $\text{Mg}_2\text{TiO}_4$ ), baddeleyite ( $\text{ZrO}_2$ ) and zircon ( $\text{ZrSiO}_4$ ). He inferred that rutile and zircon were detrital minerals incorporated into the original sediments, with the other three minerals having formed from the reaction of rutile and zircon with the host carbonates during contact metamorphism. The geikielite isograd, located close to CIII in Fig. 9, corresponds to the model reaction: rutile + Dol = geikielite + Cal +  $\text{CO}_2$ . The baddeleyite isograd, located close to the spinel isograd (C16) in Fig. 9, corresponds to the model reaction: zircon + Dol = baddeleyite + Fo + Cal +  $\text{CO}_2$ . The qandilite isograd, located near the periclase isograd (C15) in Fig. 9, corresponds to the model reaction: geikielite + periclase = qandilite. Ferry (1996a) showed that temperature estimates from these isograds agreed with temperature estimates using calcite–dolomite thermometry and carbonate–silicate phase equilibria.

### Contact metamorphism of quartzites

Contact metamorphic effects in the Appin Quartzite are manifested by recrystallization and grain growth of clastic quartz (Buntebarth and Voll 1991; Lind 1996), and by transitions in the structural state of clastic alkali feldspar (Kroll *et al.* 1991). 750 m from the igneous contact south of Sgorr Dhearg, Buntebarth and Voll (1991) observed that the mean diameter of quartz grains began to increase from the typical regional values of 0.2 mm, increasing to over 1.0 mm at the contact. The onset of quartz coarsening corresponds approximately to the Zone III/ Zone IV transition (*c.* 600–620°C) in interbedded pelites, and is associated with extensive removal of intragranular strain in quartz by dislocation climb and subgrain boundary movement (Lind 1996).

Kroll *et al.* (1991) examined the kinetics of disordering, re-ordering and unmixing in clastic alkali feldspar grains in the Appin Quartzite in the vicinity of the Allt Giubhsachain syncline in the NE part of the aureole. They observed three zones in the aureole: a zone unaffected by contact metamorphism, characterized by low microcline; a transitional zone between 1900 m and 1100 m from the igneous contact, in which both low microcline and orthoclase are found; and a high grade zone in which low microcline is absent and orthoclase and intermediate microcline occur. They interpreted the orthoclase and intermediate microcline to represent sanidine that re-ordered on cooling. Consequently, they placed the microcline–sanidine transition 1900 m from the igneous contacts, just outside the first development of cordierite in interbedded pelites. They estimated a temperature of about 480°C for the transition, somewhat lower than the 550–560°C estimate for the nearby cordierite isograd.

### Fluid presence and movement in the aureole

Stable isotopic evidence concerning fluid movement in the aureole

Stable isotopic measurements ( $\delta^{18}\text{O}$ ,  $\delta^{13}\text{C}$  and  $\delta\text{D}$ ) of metapelitic and metacarbonate rocks in the aureole

(Hoernes *et al.* 1991; Linklater *et al.* 1994; Ferry 1996b) show an overall pattern of variability. For pelitic and semipelitic rocks,  $\delta^{18}\text{O}$  and  $\delta\text{D}$  vary from +9.3 to +16.1‰ and –62 to –38‰, respectively. Out of 60 pelitic and semipelitic samples analyzed, 51 fall within the range  $\delta^{18}\text{O} = 11\text{--}15\text{‰}$ . For marbles from Coire Guibhsachain,  $\delta^{18}\text{O}$  and  $\delta^{13}\text{C}$  have values of  $20 \pm 2.5$  and  $3 \pm 1\text{‰}$  respectively. Isotopic variations are preserved on the centimetre-scale within and between samples of adjacent carbonate and pelite, and migmatitic leucosomes show  $\delta^{18}\text{O}$  values congruent with their immediately adjacent mesosomes, but the values for both leucosome and mesosome vary from sample to sample. These data, coupled with comparisons with country rocks outside the aureole, suggest that the compositions of the original metasediments were largely preserved during contact metamorphism and migmatization.

Several profiles from outside the aureole up to the igneous contact and into the igneous complex were examined for isotope variability by Hoernes *et al.* (1991), but no consistent patterns related to distance to the igneous contact were found. One profile in the southern part of the aureole, close to profile B in Fig. 3, shows weak evidence for lowering of  $\delta^{18}\text{O}$  within 100m of the igneous contacts, possibly due to local outward fluid migration from the intrusion. In the area of disrupted migmatites in the Chaotic Zone, Linklater *et al.* (1994) found isotopic variations consistent with some fluid infiltration from the complex, but although this was sufficient for substantial melting, the effect on isotope compositions was small.

Overall isotopic compositions and variations in the aureole provide no evidence of substantial fluid flow between rock units. As with the isotopic data from the intrusive rocks, the data argue against development of a pervasive hydrothermal convection system around the igneous complex, or for pervasive lateral fluid migration between the igneous complex and the country rocks.

### Petrological evidence concerning fluid presence and movement in the aureole

Despite the stable isotopic evidence above, mineral assemblages in pelites, siliceous carbonates and quartzites indicate locally varying extents of fluid presence and of fluid infiltration during the contact metamorphic event (Masch and Heuss-Assbichler 1991; Heuss-Assbichler and Masch 1991; Harte *et al.* 1991b; Ferry 1996b). The studies of Linklater *et al.* (1994) and Ferry (1996b) showed that fluid fluxes sufficient to provide volatiles for reactions (including melting) may have been insufficient to markedly modify bulk rock oxygen isotope ratios. In this discussion of fluid behaviour, we distinguish between *fluid presence*, by which we mean either the presence of a stagnant fluid in the pores of a rock or of a fluid generated internally by devolatilization reactions, and *fluid infiltration*, by which we mean the ingress into a rock of fluid which originated elsewhere. Owing to the vanishingly small porosity of rocks under lithostatic pressure (see below), the amount of fluid that fills that porosity will have been small compared with the amount of fluid required for the observed reactions, so that we regard the effects of a

stagnant fluid to have been relatively minor in the fluid history of the aureole (see also Ferry 1996b).

*Fluid presence and movement.* The prograde metamorphic reactions described above in pelites and siliceous carbonates are largely devolatilization reactions, such that fluid presence must commonly have occurred during heating of the aureole rocks. In particular in the abundant pelitic rocks, reactions involved in the transition from chlorite-bearing regional schists outside the aureole to relatively anhydrous pelitic hornfelses in the aureole will have resulted in the release of significant volumes of hydrous fluid. Harte *et al.* (1991b) argued, on the basis of the regularity of the pelitic isograds and their estimated temperatures, that the pelitic mineral assemblages indicate the presence of a volatile phase close to pure H<sub>2</sub>O under pressures similar to those of the solid rocks at times of reaction ( $P_{\text{H}_2\text{O}} \approx P_{\text{fluid}} = P_{\text{lithostatic}} \approx 3$  kbar). In siliceous carbonates, most of the reactions produce and/or consume H<sub>2</sub>O and CO<sub>2</sub>, indicating both the presence and mobility of mixed H<sub>2</sub>O–CO<sub>2</sub> fluids. Masch and Heuss-Assbichler (1991) and Ferry (1996a, b) argued that the H<sub>2</sub>O–CO<sub>2</sub> fluids were at lithostatic pressure during times of reaction.

The fluid generated during reaction of the pelitic and siliceous carbonate rocks must have escaped the rocks and migrated upwards and perhaps laterally through other rocks in the aureole, but such movement might have taken place along selected fractures or other channelways and therefore not have promoted isotopic homogenization in the rocks through which they passed. The extent to which fluid tends to move pervasively through the rock matrix, rather than be constrained to isolated pore volumes or restricted to movement along channelways, depends on a number of factors (Brenan 1991), including: the dihedral angles of the fluid in rocks of different composition (Watson and Brenan 1987; Holness 1995, 1997); lithological anisotropies (such as bedding planes, faults and pre-existing fractures); and, in the case of rocks generating and expelling fluids, the way in which they respond to hydraulic fracturing. Permeability of individual rock types during contact metamorphism at Ballachulish will have been influenced by the orientation of metamorphic fabrics (e.g., schistosity in pelites) and the density and orientation of discrete channelways and fractures (especially in brittle rock types such as quartzites) induced by the prior regional deformation and metamorphism.

In pelites, quartz  $\pm$  feldspar-bearing microveins first become noticeable in the recrystallized hornfelses of Zone IVb. We interpret these veins as evidence of hydraulic fracturing of the hornfels to allow the escape of fluids generated during reaction. In contrast, in the less recrystallized, lower grade rocks that partially retain the pre-contact metamorphic regional schistosity, fluid escape during reaction may have been more pervasive owing to the greater number and closer spacing of potential fluid pathways parallel to the preexisting schistosity. Heuss-Assbichler and Masch (1991) described features in siliceous carbonates in Coire Giubhsachain that they ascribed to hydraulic fracturing in response to fluid release associated with reaction C9.

*Prograde fluid infiltration.* The extent and nature of fluid infiltration into the aureole as it heated up varied from place to place. The two locations which provide the best constraints on the extent of fluid infiltration are Coire Giubhsachain on the NE flank, and in the vicinity of the Chaotic Zone on the west flank.

In Coire Giubhsachain, generally restricted fluid influx within 350 m of the contact is indicated by the localized and typically limited development of partial melting in the widespread pelitic and semipelitic rocks (see discussion above), and the similarity of  $\delta^{18}\text{O}$  in adjacent leucosome and hornfels rocks despite a wide overall variability in  $\delta^{18}\text{O}$  (Linklater *et al.* 1994). Thus, although the igneous complex was releasing fluid during crystallization, and pelites were generating hydrous fluid, these fluids do not appear to have pervasively infiltrated the rocks. In feldspar-bearing quartzites, lack of any evidence for partial melting within the high temperature contact zone, and isotopic disequilibrium between quartz and feldspar (Hoernes and Voll 1991), indicates minimal prograde fluid influx through the quartzite rock matrix, though some aspects of the kinetic studies of Buntebarth and Voll (1991) and Kroll *et al.* (1991) suggested the local, transient presence of a minimal amount of fluid. Evidence for fluid channelling in the quartzites is provided by abundant quartz veins.

Siliceous carbonate assemblages in Coire Giubhsachain (Masch and Heuss-Assbichler 1991; Ferry 1996b) indicate a transition in extent of prograde infiltration going from mid-grade to high-grade conditions. In an interval between c. 350 and 650 m from the igneous contact, the widespread occurrence of the model isobaric invariant assemblage CIII, Fo + Di + Tr + Cal + Dol, indicates fluid compositions ranging from  $X_{\text{CO}_2} = 0.5\text{--}0.9$ , depending on the effect of minor components in tremolite (Ferry 1996b). The presence of this assemblage and a number of model isobarically univariant assemblages in the same interval (Masch and Heuss-Assbichler 1991) indicates internal buffering of the fluid phase composition. Thus, although fluid was generated, there was no extensive fluid flow that homogenized fluid compositions.

In contrast, within 350 m of the igneous contacts in Coire Giubhsachain, infiltration of relatively water rich fluids is required locally for the production of wollastonite ( $X_{\text{CO}_2} < 0.5$ ) and periclase ( $X_{\text{CO}_2} < 0.1$ ) at the indicated temperature conditions (see Fig. 10). Ferry (1996b) estimated that local prograde fluid fluxes of 100 to 1000 mol cm<sup>-2</sup> were required to produce these assemblages. He inferred that the direction of fluid flow was most likely vertical and upwards, although a lateral component could not be ruled out. Infiltration of water-rich fluids in other parts of the high grade zone in Coire Giubhsachain is indicated by locally abundant grossular-bearing marble and grossular + vesuvianite-bearing calcisilicate assemblages, which are only stable at  $X_{\text{CO}_2} < 0.3$  (see Fig. 10).

Therefore, the overall evidence from metasomatic reactions in Coire Giubhsachain is that prograde fluid infiltration was generally limited rather than extensive, and channelled rather than pervasive. The greatest amount of fluid infiltration appears to have been focused in the inner

contact zone, with the most probable fluid source being pelitic rocks undergoing dehydration, although a magmatic component close to the contacts may also have been important locally.

On the west flank, extensive partial melting in the Chaotic Zone indicates widespread, although possibly not voluminous, infiltration of magmatically-derived fluid into the Leven Schist semipelites within about 400 m of the contact (Pattison and Harte 1988; Linklater *et al.* 1994). In contrast, siliceous carbonates of the Ballachulish Limestone and Appin Phyllite/Limestone lithologies immediately downgrade of the Chaotic Zone migmatites contain a range of mineral assemblages that suggest varying fluid compositions and abundances. Model invariant and univariant assemblages involving combinations of Cal, Dol, Di, Fo, Qtz and Tr are suggestive of minimal fluid infiltration (assuming the minerals are not retrograde, cf. Ferry 1996b), whereas rarer Grt- and Wo-bearing assemblages, sometimes interlayered with the former assemblages, are indicative of localized water-rich fluid infiltration (reactions C14 and C19 in Fig. 10). The contrast in behaviour between this restricted infiltration and the more widespread fluid infiltration of the adjacent Chaotic Zone migmatites may be related to permeability contrasts between the pelites and siliceous carbonates, such as: those depending on the connectivity of fluid porosity (e.g. Holness and Graham 1995; Holness 1997); and the tendency of rocks undergoing partial melting to absorb water, which creates both a chemical potential gradient and physical gradient (related to the negative volume change of vapour-consuming melting reactions; Percival 1989) that would have favoured migration of water into the semipelitic rocks.

Elsewhere in the aureole, the generally restricted amount of melting suggests that H<sub>2</sub>O supply was limited. The mineralogical assemblage evidence on fluid flow probably underestimates the overall fluid flow, owing to the potentially large amount of fluids that may have been channelled rather than pervading the metasediments. Pelitic and siliceous carbonate lithologies appear to show more mineralogical and isotopic evidence for pervasive fluid infiltration than quartzite units. Fluid paucity in the matrix of the quartzites may be attributed to some or all of: lower intrinsic permeability due to unfavourable pore shapes and fluid continuity (Holness 1995, 1997); lack of reaction-enhanced permeability in the quartzites; and the greater tendency to brittle deformation in the quartzites, the latter favouring fluid channelling.

*Retrograde conditions.* Fluid infiltration following the thermal peak is indicated by a variety of retrograde minerals in pelitic hornfelses and siliceous carbonates. In pelitic rocks a protracted history of retrogression is indicated by a range of alteration assemblages which commonly involve hydration reactions (Pattison and Harte 1991, p. 174–8). These include: replacement of cordierite by a variety of products, including intergrown muscovite, biotite and/or chlorite and fine-grained shimmer aggregates (pinitite); replacement of K-feldspar, andalusite and corundum by sericite; and chloritization of biotite. Retrograde

equivalents of many of the prograde reactions appear to have operated at least locally, indicating that retrograde fluids were present variably throughout the cooling history. Whereas retrogression, especially of cordierite, is fairly widespread and uniform at lower grades (Zones II and III), it is often more localized and patchy in rocks of Zone IV and higher, suggesting more pronounced channelling through the more recrystallized hornfelses. Extensive chlorite+sericite+pinitite retrogression of rocks from Zone IV and higher is found in the migmatites of the Chaotic Zone, and in hornfelses from the NE flank by Ballachulish Bridge, the SW flank in Glen Duror, and surrounding the satellite stock in the SE of the area (Pattison and Harte 1991).

Retrograde minerals are widespread in siliceous carbonates in Coire Giubhsachain and elsewhere in the aureole, the most common types of retrogression being the development of serpentine after forsterite, brucite after periclase, and tremolite after diopside, but retrograde dolomite, calcite and quartz are also seen (Ferry 1996b). In Coire Giubhsachain, Ferry (1996b) showed that different rock types show distinct sequences of retrograde minerals, some of which record a protracted history of retrogression over a temperature interval of c. 750–400°C. He estimated time-integrated retrograde fluid fluxes on the order of 1000 mol fluid cm<sup>-2</sup>, with locally higher values nearer to the igneous contact that he suggested might reflect fluid focusing in the inner contact zone. Although Ferry (1996b) concluded that in the sample examined retrograde fluid flow was generally pervasive and uniform, some samples from Coire Giubhsachain and other parts of the aureole show evidence of more channelled fluid movement, such as the patchy replacement of forsterite by serpentine and the occurrence of late veins.

Overall, evidence for retrograde fluid movement during cooling of the aureole as a whole appears to be widespread owing to the fact that few rocks are entirely free of retrograde minerals (cf. Ferry 1996b). On the other hand, the magnitude, uniformity and timing of this retrogression appears to have varied, and some of the observed retrogression may have occurred considerably later than the contact metamorphic event. The source and driving mechanism of the retrograde fluids is uncertain, but the variability of retrograde alteration coupled with the isotope evidence appears to eliminate significant circulation of magmatic or meteoric fluids, leaving metamorphic fluids as the most likely possibility. Thermal modelling (see below) shows that as the thermal pulse moved out into the aureole, rocks in the inner aureole were cooling. Thus, a portion of the hydrous fluids released from pelitic rocks that were heating up (either laterally or laterally and below) may have migrated towards the igneous body, passing through rocks that were at the same time cooling from their peak conditions. Such a scenario would explain the reverse operation of the prograde reactions documented above, and could additionally account for sequentially lower grade episodes of retrogression recorded by some individual samples (e.g., Pattison and Harte 1991; Ferry 1996b). In high-grade zones of the aureole, notably the extensively migmatized rocks of the Chaotic Zone,

another local source of fluids for relatively high grade retrogression may have been water released during cooling and crystallization of partial melts.

The generally limited extent of prograde and retrograde fluid infiltration at Ballachulish contrasts with the situation in some higher level (< 2 km) intrusions, such as in the Tertiary igneous province of the Scottish Hebrides, where depletion in  $^{18}\text{O}$  revealed the formation of an extensive hydrothermal circulation system involving meteoric water (Taylor and Forester 1971). The contrast may be explained partly by the greater depth (*c.* 10 km) of intrusion and metamorphism exposed at Ballachulish, this depth most likely being below that at which a network of fluid-filled cracks open to the surface can exist and thereby facilitate substantial fluid circulation by convection (Harte et al. 1991*b*).

### Thermal modelling of the aureole

#### Thermal models

Buntebarth (1991) modelled the thermal evolution of the Ballachulish Igneous Complex and aureole using constraints provided by the field studies, and compared several models with the extensive temperature estimates from the rocks. Two different emplacement histories were modelled. The first assumed that the diorite magma intruded as a cylindrical ring complex around a central block of country rock, with this core of country rock later subsiding into the granitic magma in a manner analogous to the nearby Glen Coe and Ben Nevis intrusions (the 'ring' model). The second assumed that the diorite was emplaced as a cylindrical stock, followed by emplacement of the granite magma within the non-solidified core of the diorite (the 'cylinder' model). A third model, involving a steep cone-shaped body, is not significantly different from the cylinder model.

In the modelling, Buntebarth (1991) took into consideration the following factors: variations in measured thermal diffusivity and conductivity of intrusive and metasedimentary rocks; the effects of heat absorption due to endothermic devolatilization reactions in pelitic rocks; fluid migration towards or away from the intrusion; latent heat of crystallization of the magmas; varying emplacement temperatures of the different magmas; and varying initial country rock temperatures prior to emplacement. In the ring model, heat was assumed to have been conducted outwards into the country rocks as well as inwards into the central block; whereas in the cylinder model, heat was assumed to have migrated outwards into the country rocks only.

Thermal profiles were modelled across four different parts of the aureole to take account of variations in aureole width, intrusive rock type, host rocks and host rock fabrics (transects A to D in Fig. 3). Figure 11 shows profiles of maximum temperature versus distance for the four transects. Transect A on the east flank is the best constrained area for rock temperature estimates, and was used to test different models. In general, calculated thermal profiles from the ring model (Fig. 11a) produced too steep a

drop-off of temperature away from the igneous contacts to reconcile with the isograd spacing, and absolute temperatures for all reasonable ring model conditions were too low compared to phase equilibrium constraints. In contrast, calculated thermal profiles from the cylinder model assuming no inward or outward fluid movement (conductive model) fit the relative and absolute constraints provided by the isograds well. The best models for the east flank assumed a country rock consisting entirely of quartzite, or of quartzite and pelite in a 2:1 ratio, in good agreement with the approximate proportions of host rocks observed along this flank of the aureole (Fig. 3). The estimated contact temperature of 750–800°C is in good agreement with phase equilibrium estimates from rocks near the east contact (Pattison 1991).

Modelling of thermal profiles in the NE (Fig. 11d) and south (Fig. 11b), using the cylinder model and other input parameters appropriate to the rock types concerned, yielded generally excellent agreement with the isograd and petrological temperature constraints. The narrower width of the aureole in the southern profile (Fig. 11b) compared to the eastern profile (Fig. 11a) for similar intrusion temperatures can be accounted for by the higher proportion of quartzite in the eastern area. A combination of relatively high heat conductivity and lack of endothermic reactions in quartzite allowed heat to be conducted outwards through the quartzites into the country rocks more effectively than through the more reactive pelitic rocks. The especially narrow width of the aureole in the NE (Fig. 11d) is accounted for by the relatively low temperature phase of the intrusive complex in this area (*c.* 1000°C), combined with country rocks consisting entirely of reactive, heat-consuming pelitic rocks.

The one thermal profile that was poorly fitted was in the SE (Fig. 11c), where regardless of the model parameters used, calculated thermal profiles could not reproduce qualitatively or quantitatively the pattern of isograd constraints. In this part of the aureole, petrological and geophysical evidence indicates that the intrusion bulges outwards shallowly under the exposed metasediments to connect with the small stock to the SE, most likely causing the elevated thermal structure indicated by the isograds.

#### Thermal evolution of the aureole

The thermal modelling of Buntebarth (1991) allows the construction of temperature–time ( $T-t$ ) paths for rocks at different distances from the contact, allowing an understanding of the dynamic evolution of the contact metamorphic event. Figure 12 shows a series of  $T-t$  paths for rocks at different distances from the contact assuming instantaneous emplacement of the intrusion (cylinder model) into the Appin Quartzite at a pre-intrusion temperature of 250°C (corresponding to Fig. 11a). Although different emplacement scenarios show different absolute values, the resultant patterns of thermal evolution are similar and the estimated duration of events is of a similar order to that shown in Figure 12.

The thermal modelling shows that intrusion of the later granite had no effect on maximum temperatures reached

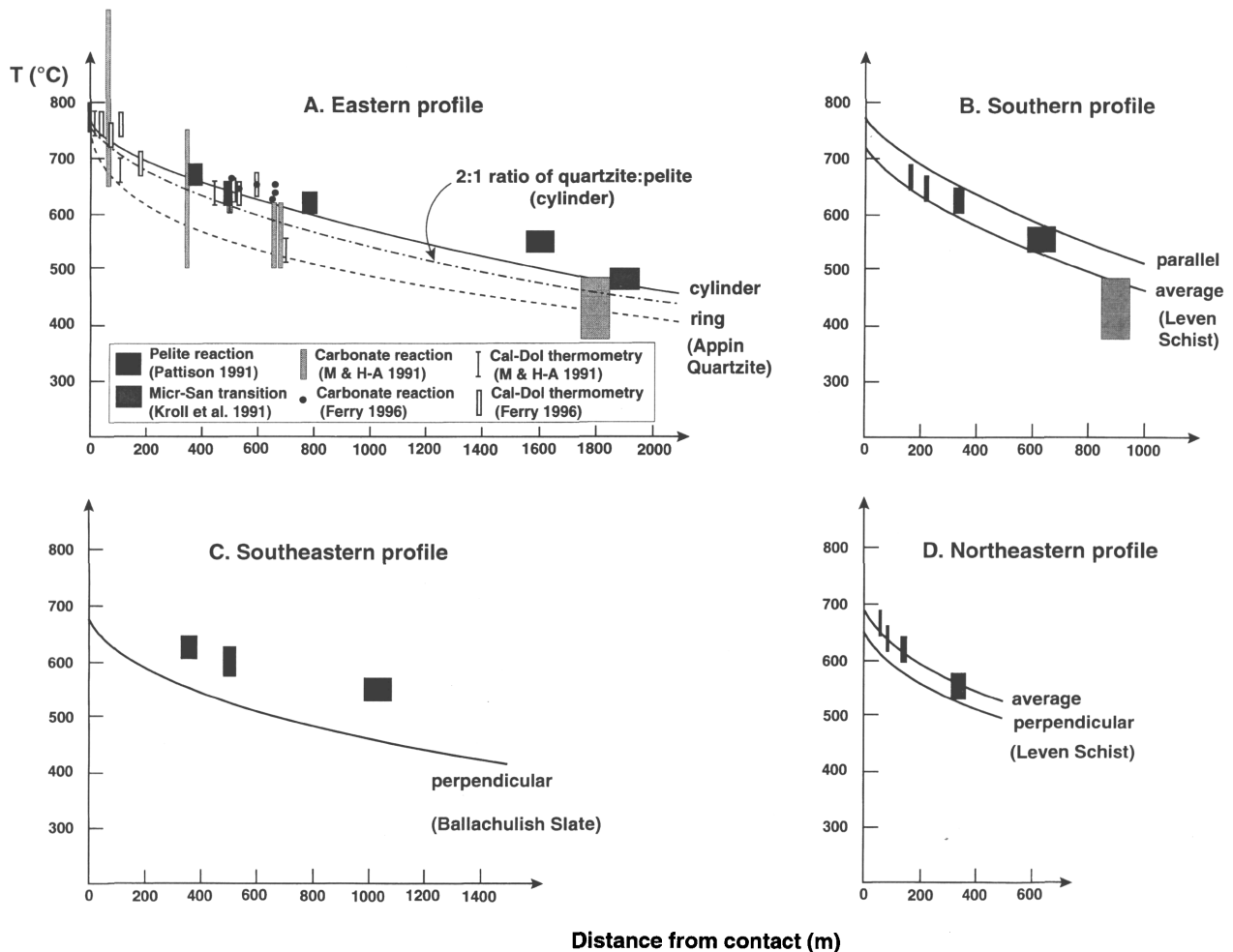


FIG. 11. Thermal profiles of maximum (time-integrated) temperature versus distance from the contact (Buntebarth 1991), compared with petrological temperature constraints (see compilation in Pattison 1991 and Ferry 1996a). All modelled profiles assume: the cylinder model (except for the short dashed profile in (a) which is for the ring model); a pre-intrusion country rock temperature of 250 °C; an intrusion temperature of 1050 °C (except in profile D where 1000 °C); no fluid movement; and operation of endothermic reactions in pelitic rocks. (a) Eastern transect, showing thermal profiles for the cylinder and ring models (respectively, solid and dashed lines) assuming a country rock consisting of Appin Quartzite, and for the cylinder model assuming a 2:1 ratio of quartzite:pelite (dot-dash line). (b) Southern profile, with igneous contact perpendicular to the regional schistosity in the Leven Schist; the two profiles are for average thermal conductivity and diffusivity values for the host schists, and thermal values parallel to the schistosity. (c) Southeastern profile, with igneous contacts parallel to regional schistosity in the Ballachulish Slate lithology; see text for discussion of mismatch between thermal model and isograd temperatures. (d) North-eastern transect, with igneous contacts parallel to the regional schistosity in the Leven Schist; the two profiles are for average thermal conductivity and diffusivity values for the host schists; and thermal values perpendicular to the schistosity.

in the aureole and little effect on  $T-t$  paths. A slight bulge in the  $T-t$  path for rocks at the contact (0 m) is detectable in the interval between about 150 and 500 ka, but this effect becomes negligible at distances greater than 300 m from the contact. The minor effect of the granite intrusion on the thermal evolution of the aureole is most likely due to its relatively low temperature (*c.* 850 °C) and its emplacement shortly after that of the diorites (see above).

Figure 12 shows that rocks close to the contact will have reached their maximum temperature earlier, and will have experienced faster heating rates, than those farther out in the aureole. Thus, the profiles of maximum temperatures versus distance (Fig. 11 and inset to Fig. 12) are time-integrated profiles and do not correspond to thermal profiles that existed in the aureole at any given time. Rocks successively farther out in the aureole will have been heating up

while at the same time rocks closer to the contact will have been cooling from their thermal peak. A notable feature of Figure 12 is that, with the exception of the innermost aureole, the thermal maxima are broad. Consequently, most of the aureole rocks spent a relatively long time (50–100 ka) near their thermal maximum, favouring equilibration near the thermal maximum.

Superimposed on the  $T-t$  paths are the locations of the equilibrium conditions for the main pelitic isograd reactions in the aureole. An isograd in the field specifies the outermost location where the conditions for the isograd reaction have been attained, and is where the slowest heating rates possible for the reaction to proceed occur. Assuming negligible kinetic overstep, the time at which an isograd was established ('frozen in' to the rocks) corresponds to the horizontal tangent of the  $T-t$  path whose

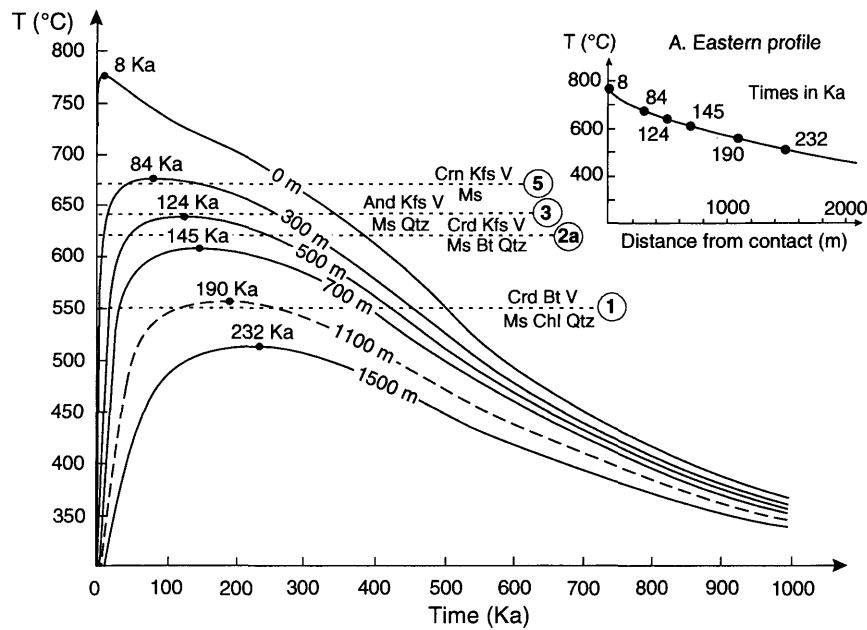


FIG. 12. Temperature–time ( $T-t$ ) paths for different distances from the contact (compiled from Buntebarth 1991 and Heuss-Assbichler and Masch 1991), assuming: the cylinder model; host rocks of Appin Quartzite; pre-intrusion country rock temperature of 250°C; intrusion temperature of 1050°C; no fluid movement. The dashed  $T-t$  path for 1100 m is interpolated from the other data. Horizontal dashed lines, temperatures of selected pelitic isograd reactions. Inset diagram shows the time-integrated profile of maximum temperatures versus distance from Fig. 11A, with times at which the maximum temperature was attained taken from the main diagram.

maximum temperature is that of the inception of the isograd reaction in question. For example, the  $\text{Ms} + \text{Qtz} = \text{And} + \text{Kfs}$  isograd (P3;  $c. 640^\circ\text{C}$ ) will have been established approximately 120 ka after intrusion at a distance slightly less than 500 m from the contact. Whereas the corundum isograd (P5;  $c. 670^\circ\text{C}$ ) will have been established at about 90 ka, the cordierite isograd (P1;  $c. 550^\circ\text{C}$ ) will not have been established until about 200 ka.

Contrasting with the final establishment of a given isograd is the progress of the isograd reaction as a function of time and distance from the contact. Rocks progressively closer to the contact will have passed through the temperature threshold for a given isograd reaction progressively earlier and at progressively faster rates. For example, rocks 300 m from the contact will have exceeded the  $c. 550^\circ\text{C}$  threshold for the cordierite isograd (P1) less than about 5 ka after intrusion, compared to  $c. 20$  ka for rocks 700 m from the contact and 200 ka for rocks at the isograd ( $c. 1100$  m according to the model). Thus, the isograd as examined in the field represents the latest time of reaction rather than the beginning of reaction, as is sometimes assumed. Through time, isograds will therefore have emanated outwards from the intrusion in a similar manner to isotherms (Lasaga 1986).

The overall duration of the contact metamorphic event in terms of the time that rocks that were heated to temperatures above the cordierite isograd ( $c. 550^\circ\text{C}$ ) was about 500 ka (Fig. 12). For rocks upgrade of the isograd, the majority of this time will have been spent cooling down to this temperature from higher temperature conditions. The time during which rocks were hot enough to be partially molten (temperatures exceeding the threshold of vapour-consuming melting described by reaction P7,  $c. 660^\circ\text{C}$ ) was about

270 ka. These times are all based on the models shown in Figure 12 and probably represent minimum times, owing to the fact that the assumed instantaneous emplacement of the intrusion is geologically unlikely. A more gradual rise of temperature as the intrusion reached its level of emplacement is to be expected, leading to a longer contact metamorphic duration and slower heating rates than those predicted by Fig. 12, especially in the inner part of the aureole.

### Equilibrium and kinetic controls on reaction progress and isograd development

The distribution of isograds and temperature estimates in interlayered lithologies allows an assessment of the relative role of kinetics and equilibrium in controlling isograd development in the aureole (Pattison 1991). In this discussion, we note the distinction between overstepping of isograds and overstepping of reactions (see above). Walther and Wood (1984) argued that overstepping of devolatilization reactions (and by extension isograds), in which reaction occurs by a solution–precipitation process in the presence of a fluid phase, would be minimal under most natural conditions (including those of contact metamorphism). On the other hand, they suggested that overstepping of solid–solid reactions such as  $\text{And} = \text{Sil}$  could be appreciable in contact metamorphic environments. In contrast, Lasaga (1986) and Lasaga and Rye (1993) have suggested that most reaction isograds, especially in contact aureoles, are in fact ‘kinetic’ reaction isograds whose progress and location may be quite different than those predicted by equilibrium models.

In the Ballachulish Aureole, the sequence and spacing of isograds within single lithologies (e.g., pelites, siliceous

carbonates), and between them where in close proximity (e.g., Coire Guibhsacahin), are consistent with predictions from equilibrium models (compare Figs. 3 and 7, and 9 and 10). Temperature estimates within and between lithologies are in excellent agreement (Fig. 11a; Pattison 1991; Ferry 1996a). Mineral compositions in pelites within metamorphic zones vary smoothly as a function of grade and satisfy equilibrium models involving continuous and discontinuous reactions (Pattison 1991). Apart from the distribution of andalusite and sillimanite, no unusually low variance assemblages, which would be suggestive of reaction overstepping, are found in pelites in the main aureole (exceptions may occur in the narrow aureole surrounding the small satellite intrusion in the southeast; Pattison 1985, 1991). Interpretation of assemblages in siliceous carbonates is less clear, owing to the fact that fluid infiltration was required to drive some of these reactions and the occurrence of retrograde minerals complicates interpretation of peak assemblages (Ferry 1996b).

The above patterns occur even though heating rates varied in the aureole and the different lithologies show wide variations in mineralogy, grain size and fluid composition, all of which have been shown to influence reaction kinetics at laboratory time scales (Kerrick *et al.* 1991). If kinetics significantly influenced isograd development in the Ballachulish aureole, one would expect a less consistent pattern of isograds and temperature estimates than is seen. Regarding predictions of overstepping of cordierite isograds by Putnis and Holland (1986), the agreement between the sequence and spacing of pelitic isograds in the field, some of which involve cordierite and others which do not, with the equilibrium phase diagram (Fig. 7) argues against this effect (Pattison 1991; Maresch *et al.* 1991).

Overall, most of the evidence from the aureole suggests that an equilibrium model is satisfactory in accounting for the isograd patterns. By 'equilibrium' we mean that most rocks in the aureole developed the stable (equilibrium) mineral assemblage appropriate to the maximum temperature they attained. This situation will have been favoured by the relatively long time the rocks spent near their thermal maximum (see above). However, the above does not imply or necessitate that all rocks achieved their final maximum temperature assemblages by proceeding along paths of equilibrium mineral assemblage development at all times during heating. Kinetic factors must be expected to have been more important in controlling the initial progress of isograd reactions close to the contacts where heating rates were fastest. For example, rocks 300 m from the contact will have passed through the temperature threshold for reactions P1, P2a, P3 in less than 15 ka before reaching their maximum temperature slightly above isograd reaction P5 at about 84 ka.

Unfortunately, evidence for possible kinetic control on low grade reactions in rocks that were heated to higher temperatures is difficult to obtain because textural and compositional features developed during the low grade reactions tend to be obliterated by the effects of later reactions and by the general tendency of rocks to recrystallize

as temperature rises. A possible exception to this situation, involving the  $Tr + Dol = Fo + Cal$  isograd reaction C9, was discussed by Heuss-Assbichler and Masch (1991). They used microstructural patterns combined with thermal modelling to argue for increasing degrees of overstepping of the reaction from essentially 0°C in the vicinity of the isograd, c. 700 m from the contact, to as much as 50°C, 230 m from the contact. Ferry (1996a, b) questioned some aspects of this interpretation, finding that tremolite in the rocks he examined from the same interval was of retrograde rather than prograde origin. This difference in interpretation brings out a general problem, that assemblage and compositional features which might be attributed to kinetic control during prograde metamorphism may also be a product of limited retrogression and resetting during cooling.

Prograde reactions whose progress definitely appears to have been dominated by kinetic factors mainly relate to solid–solid reactions and to intracrystalline processes. The distribution and mode of occurrence of sillimanite, and therefore the andalusite–sillimanite transition, with its very low free energy of transformation, is clearly controlled by kinetic factors (see above and Pattison, 1992). Masch and Heuss-Assbichler (1991) argued that calcite–dolomite thermometry only records temperatures at isograds rather than between isograds, owing to the sluggishness of equilibration of Cal and Dol at times other than when the two minerals were involved in a solution–precipitation (reaction) process, although Ferry (1996a, b) found that Cal–Dol temperatures were consistent with other phase equilibrium constraints regardless of position with respect to isograds. Feldspar ordering shows evidence for overstepping of the equilibrium transitions (Kroll *et al.* 1991), while feldspar and quartz in the Appin Quartzite show a sluggish approach to stable isotopic equilibrium (Hoernes and Voll 1991).

The above features in the quartzites may be attributed not only to the nature of the transformations involved, but also to the limited presence of a fluid phase in this lithology. In general for the Ballachulish aureole rocks, substantial equilibrium always seems to have been approached when a fluid phase was clearly present, not only to participate in reactions but to act as a catalyst by aiding diffusion and other atomic transport processes. This observation is consistent with experimental studies which show that reaction rates under fluid-present conditions are orders of magnitude faster than under fluid-absent conditions (Rubie 1986).

### Acknowledgements

We thank Dr. S. Weiss, Dr. S. Heuss-Assbichler and Dr. J. M. Ferry for reviewing parts of an early draft of the paper, and Dr. T. J. Dempster and an anonymous Journal reviewer for their comments which led to significant improvements in the presentation of the paper. Diane Baty is thanked for drafting the maps. D.R.M.P. used funds from his Natural Sciences and Engineering Research Council of Canada grant 0037233 to support this work.

## References

- ANDERSON, J. G. C. 1956. The Moian and Dalradian rocks between Glen Roy and the Monadhliath mountains. *Transactions of the Royal Society of Edinburgh* **63**, 15–36.
- ASHWORTH, J. R. 1985. Introduction. In Ashworth, J. R. (ed.), *Migmatites*. Blackie, Glasgow, 1–35.
- ATHERTON, M. P. 1977. The metamorphism of the Dalradian rocks of Scotland. *Scottish Journal of Geology* **13**, 331–70.
- BAILEY, E. B. 1923. The metamorphism of the southwestern Highlands of Scotland. *Geological Magazine* **60**, 317–31.
- and MAUFE, H. B. 1916 (first edition); 1960 (second edition). *The geology of Ben Nevis and Glen Coe and the surrounding country: Explanation of Sheet 53. Memoirs of the Geological Society of Scotland*. Her Majesty's Stationery Office, Edinburgh.
- BERMAN, R. G. 1988. Internally consistent thermodynamic data for stoichiometric minerals in the system  $\text{Na}_2\text{O}-\text{K}_2\text{O}-\text{CaO}-\text{MgO}-\text{FeO}-\text{Fe}_2\text{O}_3-\text{Al}_2\text{O}_3-\text{SiO}_2-\text{TiO}_2-\text{H}_2\text{O}-\text{CO}_2$ . *Journal of Petrology* **29**, 445–522.
- BOWES, D. R. and WRIGHT, A. E. 1967. The explosion-breccia pipes near Kentallen, Scotland, and their geological setting. *Transactions of the Royal Society of Edinburgh* **67**, 109–141.
- BRENAN, J. M. 1991. Development of metamorphic permeability: implications for fluid transport processes. In Kerrick, D.M. (ed.), *Contact metamorphism*. Mineralogical Society of America, Reviews in Mineralogy **26**, 291–320.
- BUNTEBARTH, G. 1991. Thermal models of cooling. In Voll, G., Töpel, J., Pattison, D. R. M. and Seifert, F. (eds.), *Equilibrium and kinetics in contact metamorphism: The Ballachulish Igneous Complex and its aureole*, 379–404. Springer Verlag, Heidelberg.
- and VOLL, G. 1991. Quartz grain coarsening by collective crystallization in contact quartzites. In Voll, G., Töpel, J., Pattison, D. R. M. and Seifert, F. (eds.), *Equilibrium and kinetics in contact metamorphism: The Ballachulish Igneous Complex and its aureole*, 251–66. Springer Verlag, Heidelberg.
- CARRINGTON, D. P. and HARLEY, S. L. 1995. Partial melting and phase relations in high-grade metapelites: an experimental petrogenetic grid in the KFMASH system. *Contributions to Mineralogy and Petrology* **120**, 270–91.
- DEMPSTER, T. J. 1985. Uplift patterns and orogenic evolution in the Scottish Dalradian. *Journal of the Geological Society, London* **142**, 111–28.
- DROOP, G. T. R. and TRELOAR, P. J. 1981. Pressures of metamorphism in the thermal aureole of the Etive Granite Complex. *Scottish Journal of Geology* **17**, 85–102.
- ELLES, G. L. and TILLEY, C. E. 1930. Metamorphism in relation to structure in the Scottish Highlands. *Transactions of the Royal Society of Edinburgh* **56**, 621–46.
- FERRY, J. M. 1996a. Three novel isograds in metamorphosed siliceous dolomites from the Ballachulish aureole, Scotland. *American Mineralogist* **81**, 485–94.
- 1996b. Prograde and retrograde fluid flow during contact metamorphism of siliceous carbonates from the Ballachulish aureole, Scotland. *Contributions to Mineralogy and Petrology*, **124**, 235–54.
- FETTES, D. J., LONG, C. B., BEVINS, R. E., MAX, M. D., OLIVER, G. J. H., PRIMMER, T. J., THOMAS, L. J. and YARDLEY, B. W. D. 1985. Grade and time of metamorphism in the Caledonian Orogen of Britain and Ireland. In Harris, A.L. (ed.), *The Nature and Timing of Orogenic Activity in the Caledonian Rocks of the British Isles*. Geological Society, London, Memoirs **9**, 41–53.
- HARTE, B. 1988. Lower Palaeozoic metamorphism in the Moine–Dalradian belt of the British Isles. In Harris, A.L. and Fettes, D.J. (eds.), *The Caledonian–Appalachian Orogen*. Geological Society, London, Special Publications, **38**, 123–34.
- PATTISON, D. R. M. and LINKLATER, C. M. 1991a. Field relations and petrography of partially melted pelitic and semi-pelitic rocks. In Voll, G., Töpel, J., Pattison, D. R. M. and Seifert, F. (eds.), *Equilibrium and kinetics in contact metamorphism: The Ballachulish Igneous Complex and its aureole*, 181–210. Springer Verlag, Heidelberg.
- , —, HEUSS-ASSBICHLER, S., HOERNES, S., MASCH, L. and WEISS, S. 1991b. Evidence of fluid phase behaviour and controls in the intrusive complex and its aureole. In Voll, G., Töpel, J., Pattison, D. R. M. and Seifert, F. (eds.), *Equilibrium and kinetics in contact metamorphism: The Ballachulish Igneous Complex and its aureole*, 405–22. Springer Verlag, Heidelberg.
- and VOLL, G. 1991. The setting of the Ballachulish intrusive igneous complex in the Scottish Highlands. In Voll, G., Töpel, J., Pattison, D. R. M. and Seifert, F. (eds.), *Equilibrium and kinetics in contact metamorphism: The Ballachulish Igneous Complex and its aureole*, 3–17. Springer Verlag, Heidelberg.
- HASLAM, H. W. and KIMBELL, G. S. 1981. *Disseminated copper-molybdenum mineralisation near Ballachulish, Highland region*. Mineral Reconnaissance Programme Report, Institute of Geological Sciences (U.K.) **43**, 1–42.
- HEUSS-ASSBICHLER, S. 1987. *Mikrotexturen, Reaktionsmechanismen und Stofftransport bei Dekarbonatisierungsreaktionen in Thermo-aureolen*. Ludwig-Maximilians-Universität, München, Ph.D. thesis (unpublished).
- and MASCH, L. 1991. Microtextures and reaction mechanisms of carbonate rocks: a comparison between the thermo-aureoles of Ballachulish and Monzoni (N. Italy) In Voll, G., Töpel, J., Pattison, D. R. M. and Seifert, F. (eds.), *Equilibrium and kinetics in contact metamorphism: The Ballachulish Igneous Complex and its aureole*, 229–49. Springer Verlag, Heidelberg.
- HICKMAN, A. H. 1975. The stratigraphy of late Precambrian metasediments between Glen Roy and Lismore. *Scottish Journal of Geology* **14**, 191–212.
- HOERNES, S. and VOLL, G. 1991. Detrital quartz and K-feldspar in quartzites as indicators of oxygen isotope exchange kinetics. In Voll, G., Töpel, J., Pattison, D. R. M. and Seifert, F. (eds.), *Equilibrium and kinetics in contact metamorphism: The Ballachulish Igneous Complex and its aureole*, 315–26. Springer Verlag, Heidelberg.
- MACLEOD-KINSELL, S., HARMON, R. S., PATTISON, D. R. M. and STRONG, D. F. 1991. Stable isotope geochemistry on the intrusive Complex and its metamorphic aureole. In Voll, G., Töpel, J., Pattison, D. R. M. and Seifert, F. (eds.), *Equilibrium and kinetics in contact metamorphism: The Ballachulish Igneous Complex and its aureole*, 351–78. Springer Verlag, Heidelberg.
- HOLDAWAY, M. J. 1971. Stability of andalusite and the aluminum silicate phase diagram. *American Journal of Science* **271**, 175–98.
- HOLNESS, M. B. 1995. The effect of feldspar on quartz– $\text{H}_2\text{O}-\text{CO}_2$  dihedral angles at 4 kbar, with consequences for the behaviour of aqueous fluids in migmatites. *Contributions to Mineralogy and Petrology* **118**, 356–64.
- 1997. Contrasting rock permeability in the aureole of the Ballachulish Igneous Complex, Scottish Highlands: the influence of surface energy. *Contributions to Mineralogy and Petrology* in press.
- and GRAHAM, C. M. 1995. P-T-X effects on equilibrium carbonate– $\text{H}_2\text{O}-\text{CO}_2-\text{NaCl}$  dihedral angles: constraints on carbonate permeability and the role of deformation during fluid infiltration. *Contributions to Mineralogy and Petrology* **119**, 301–13.
- JACQUES, J. M. and REAVY, R. J. 1994. Caledonian plutonism and major lineaments in the SW Scottish Highlands. *Journal of the Geological Society, London* **151**, 955–69.
- JOHNSON, M. R. W. and FROST, R. T. C. 1977. Fault and lineament patterns in the southern highlands of Scotland. *Geologie en Mijnbouw* **56**, 287–94.
- KERRICK, D. M., LASAGA, A. and RAEBURN, S. P. 1991. Kinetics of heterogeneous reactions. In Kerrick, D.M. (ed.), *Contact metamorphism*. Mineralogical Society of America Reviews in Mineralogy **26**, 583–672.

- KRETZ, R. 1983. Symbols for rock-forming minerals. *American Mineralogist* **68**, 277–279.
- KROLL, H., KRAUSE, C. and VOLL, G. 1991. Disorder, re-ordering and unmixing in alkali feldspars from contact metamorphosed quartzites. In Voll, G., Töpel, J., Pattison, D.R.M. and Seifert, F. (eds.), *Equilibrium and kinetics in contact metamorphism: The Ballachulish Igneous Complex and its aureole*, 267–96. Springer Verlag, Heidelberg.
- LASAGA, A. C. 1986. Metamorphic reaction rate laws and development of isograds. *Mineralogical Magazine* **50**, 359–73.
- and RYE, D. M. 1993. Fluid flow and chemical reaction kinetics in metamorphic systems. *American Journal of Science* **293**, 361–404.
- LIND, A. 1996. *Microstructural stability and the kinetics of textural evolution*. University of Leeds, Ph.D. thesis (unpublished).
- LINKLATER, C. M. 1990. *Partial melting in the Ballachulish aureole*. University of Edinburgh Ph.D. thesis (unpublished).
- , HARTE, B. and FALLICK, A. E. 1994. A stable isotope study of the migmatitic rocks in the Ballachulish contact aureole, Scotland. *Journal of Metamorphic Geology* **12**, 273–83.
- LITHERLAND, M. 1980. The stratigraphy of the Dalradian rocks around Loch Creran, Argyll. *Scottish Journal of Geology* **16**, 105–23.
- 1982. The structure of the Loch Creran Dalradian and a new model for the SW Highlands. *Scottish Journal of Geology* **18**, 205–25.
- MACCULLOCH, J. 1817. Observations on the mountain Cruachan in Argyllshire, with some remarks on the surrounding country. *Transactions of the Geological Society* **4**, 117–38.
- MACKNIGHT, T. 1821. Mineralogical notes and observations. *Memoirs of the Wernerian Natural History Society* **3**, 104–22.
- MARESCHE, W. V., BLÜMEL, P. and SCHREYER, W. 1991. A search for variations in the structural state of cordierite in contact metamorphosed pelites. In Voll, G., Töpel, J., Pattison, D. R. M. and Seifert, F. (eds.), *Equilibrium and kinetics in contact metamorphism: The Ballachulish Igneous Complex and its aureole*, 297–314. Springer Verlag, Heidelberg.
- MASCH, L. and HEUSS-ASSBICHLER, S. 1991. Decarbonation reactions in siliceous dolomites and impure limestone. In Voll, G., Töpel, J., Pattison, D. R. M. and Seifert, F. (eds.), *Equilibrium and kinetics in contact metamorphism: The Ballachulish Igneous Complex and its aureole*, 211–28. Springer Verlag, Heidelberg.
- PATTISON, D. R. M. 1985. *Petrogenesis of pelitic rocks in the Ballachulish thermal aureole*. University of Edinburgh Ph.D. thesis (unpublished).
- 1987. Variations in Mg/(Mg+Fe), F, and (Fe,Mg) Si = 2Al in pelitic minerals in the Ballachulish thermal aureole, Scotland. *American Mineralogist* **72**, 255–72.
- 1989. P-T conditions and the influence of graphite on pelitic phase relations in the Ballachulish aureole, Scotland. *Journal of Petrology* **30**, 1219–44.
- 1991. P-T-a(H<sub>2</sub>O) conditions in the thermal aureole. In Voll, G., Töpel, J., Pattison, D.R.M. and Seifert, F. (eds.), *Equilibrium and kinetics in contact metamorphism: The Ballachulish Igneous Complex and its aureole*, 327–50. Springer Verlag, Heidelberg.
- 1992. Stability of andalusite and sillimanite and the Al<sub>2</sub>SiO<sub>5</sub> triple point: constraints from the Ballachulish aureole, Scotland. *Journal of Geology* **100**, 423–46.
- and HARTE, B. 1985. A petrogenetic grid for pelites in the Ballachulish aureole and other Scottish thermal aureoles. *Journal of the Geological Society of London* **142**, 7–28.
- and — 1988. Evolution of structurally contrasting anatectic migmatites in the 3 kbar Ballachulish aureole, Scotland. *Journal of Metamorphic Geology* **6**, 475–94.
- and — 1991. Petrography and mineral chemistry of pelites. In Voll, G., Töpel, J., Pattison, D. R. M. and Seifert, F. (eds.), *Equilibrium and kinetics in contact metamorphism: The Ballachulish Igneous Complex and its aureole*, 135–80. Springer Verlag, Heidelberg.
- and — 1994. Overview of the Ballachulish Igneous Complex, Dalradian host rocks and contact metamorphic hornfels. In Harte, B. (ed.), *Field trips for the 4th V.M. Goldschmidt International Geochemistry Conference*, 28–46. University of Edinburgh.
- and TRACY, R. J. 1991. Phase equilibria and thermobarometry of metapelites. In Kerrick, D. M. (ed.), *Contact metamorphism*. Mineralogical Society of America, Reviews in Mineralogy **26**, 105–206.
- and VOLL, G. 1991. Regional geology of the Ballachulish area. In Voll, G., Töpel, J., Pattison, D. R. M. and Seifert, F. (eds.), *Equilibrium and kinetics in contact metamorphism: The Ballachulish Igneous Complex and its aureole*, 19–8. Springer Verlag, Heidelberg.
- PERCIVAL, J. A. 1989. Melt-induced fluid pumping and the source of CO<sub>2</sub> in granulites. In Bridgwater, D. (ed.), *Fluid Movements – Element Transport and the Composition of the Deep Crust*, 61–9. Kluwer Academic Publishers.
- PITCHER, W. 1982. Granite type and tectonic environment. In Hsu, K. (ed.), *Mountain building processes*, 19–40. Academic Press, London.
- PUTNIS, A. and HOLLAND, T. J. B. 1986. Sector trilling in cordierite and equilibrium overstepping in metamorphism. *Contributions to Mineralogy and Petrology* **93**, 265–72.
- RABEL, W. and MEISSNER, R. 1991. The shape of the intrusion based on geophysical data. In Voll, G., Töpel, J., Pattison, D.R.M. and Seifert, F. (eds.), *Equilibrium and kinetics in contact metamorphism: The Ballachulish Igneous Complex and its aureole*, 121–34. Springer Verlag, Heidelberg.
- RICHARDSON, S. W., GILBERT, M. C. and BELL, P. M. 1969. Experimental determination of kyanite-andalusite and andalusite-sillimanite equilibria: the aluminum silicate triple point. *American Journal of Science* **267**, 259–72.
- ROBERTS, J. L. 1976. The structure of the Dalradian rocks in the north Ballachulish district of Scotland. *Journal of the Geological Society, London* **132**, 139–54.
- and TREAGUS, J.E. 1977. The Dalradian rocks of the Loch Leven area. *Scottish Journal of Geology* **13**, 165–84.
- ROGERS, G., DEMPSTER, T. J., BLUCK, B. J. and TANNER, P. W. G. 1989. A high precision U–Pb age for the Ben Vuirich granite: Implications for the evolution of the Scottish Dalradian Supergroup. *Journal of the Geological Society, London* **146**, 789–98.
- and DUNNING, G. R. 1991. Geochronology of appinitic and related granitic magmatism in the W Highlands of Scotland: constraints on the timing of transcurrent fault movement. *Journal of the Geological Society, London* **148**, 17–27.
- RUBIE, D. C. 1986. The catalysis of mineral reactions by water and restrictions on the presence of aqueous fluid during metamorphism. *Mineralogical Magazine* **50**, 399–415.
- SCHREYER, W. 1966. Synthetische und natürliche Cordierite. III. Polymorphiebeziehungen. *Neues Jahrbuch für Mineralogie Abh.* **105**, 211–44.
- STEPHENS, W. E. and HALLIDAY, A. N. 1984. Geochemical contrasts between late Caledonian granitoid plutons of northern, central and southern Scotland. *Transactions of the Royal Society of Edinburgh, Earth Sciences* **75**, 259–73.
- TANNER, P. W. G. 1995. New evidence that the Lower Cambrian Leny Limestone at Callander, Perthshire, belongs to the Dalradian Supergroup, and a reassessment of the 'exotic' status of the Highland Border Complex. *Geological Magazine* **132**, 473–83.
- TAYLOR, H. P. and FORESTER, R. W. 1971. Low-<sup>18</sup>O igneous rocks from the intrusive complexes of Skye, Mull and Ardnurchan, west of Scotland. *Journal of Petrology* **12**, 465–97.
- THIRWALL, M. F. 1988. Geochronology of the late Caledonian magmatism in northern Britain. *Journal of the Geological Society, London* **145**, 951–67.
- THOMPSON, A.B. 1982. Dehydration melting of pelitic rocks and the generation of H<sub>2</sub>O-undersaturated granitic liquids. *American Journal of Science* **282**, 1567–95.

- THORNTON, C. P. and TUTTLE, O. F. 1960. Chemistry of igneous rocks: I. Differentiation index. *American Journal of Science* **258**, 664–84.
- TREAGUS, J. E. 1991. Fault displacements in the Dalradian of the Central Highlands. *Scottish Journal of Geology* **27**, 135–45.
- TROLL, G. and WEISS, S. 1991. Structure, petrography and emplacement of plutonic rocks. In Voll, G., Töpel, J., Pattison, D. R. M. and Seifert, F. (eds.), *Equilibrium and kinetics in contact metamorphism: The Ballachulish Igneous Complex and its aureole*, 39–66. Springer Verlag, Heidelberg.
- VAN DER MOLEN, I. and PATERSON, M. S. 1979. Experimental deformation of partially melted granite. *Contributions to Mineralogy and Petrology* **70**, 299–318.
- VIELZEUF, D. and MONTEL, J. M. 1994. Partial melting of metagreywackes. Part I. Fluid-absent experiments and phase relationships. *Contributions to Mineralogy and Petrology* **117**, 375–93.
- VOLL, G., TÖPEL, J., PATTISON, D. R. M. and SEIFERT, F. (eds.) 1991. *Equilibrium and kinetics in contact metamorphism: The Ballachulish Igneous Complex and its aureole*. Springer Verlag, Heidelberg.
- WALTHER, J. V. and WOOD, B. J. 1984. Rate and mechanism in prograde metamorphism. *Contributions to Mineralogy and Petrology* **88**, 246–59.
- WATSON, E. B. and BRENNAN, J. M. 1987. Fluids in the lithosphere, I. Experimentally-determined wetting characteristics of CO<sub>2</sub>–H<sub>2</sub>O fluids and their implications for fluid transport, host-rock physical properties and fluid inclusion formation. *Earth and Planetary Science Letters* **85**, 497–515.
- WEISS, S. 1986. *Petrogenese des Intrusivkomplexes von Ballachulish, Westschottland: Kristallisationsverlauf in einen zonierten Kaledonischen Pluton*. Ludwig–Maximilians–Universität, München, Ph.D. thesis (unpublished).
- 1991. Nucleation and growth of pyroxene in the hypersthene diorites. In Voll, G., Töpel, J., Pattison, D. R. M. and Seifert, F. (eds.), *Equilibrium and kinetics in contact metamorphism: The Ballachulish Igneous Complex and its aureole*, 97–104. Springer Verlag, Heidelberg.
- and Troll, G. 1989. The Ballachulish Igneous Complex, Scotland: Petrography, mineral chemistry and order of crystallisation in the monzodiorite-quartz diorite suite and in the granite. *Journal of Petrology* **30**, 1069–1116.
- and — 1991. Thermal conditions and crystallisation sequence in the Ballachulish Complex. In Voll, G., Töpel, J., Pattison, D. R. M. and Seifert, F. (eds.), *Equilibrium and kinetics in contact metamorphism: The Ballachulish Igneous Complex and its aureole*, 67–98. Springer Verlag, Heidelberg.
- WRIGHT, A. E. and BOWES, D. R. 1979. Geochemistry of the Appinite suite. In Harris, A. L., Holland, C. M. and Leake, B. E. (eds.), *Caledonides of the British Isles – reviewed*. Geological Society of London Special Publications **8**, 699–704.

*MS. accepted for publication 20th December 1996*